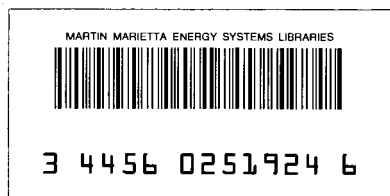


ornl

OAK
RIDGE
NATIONAL
LABORATORY



OPERATED BY
UNION CARBIDE CORPORATION
FOR THE UNITED STATES
DEPARTMENT OF ENERGY



ORNL/TM-8579

Cement-Based Radioactive Waste Hosts Formed Under Elevated Temperatures and Pressures (FUETAP Concretes) for Savannah River Plant High-Level Defense Waste

L. R. Dole
G. C. Rogers
M. T. Morgan
D. P. Stinton
J. H. Kessler
S. M. Robinson
J. G. Moore

OAK RIDGE NATIONAL LABORATORY

CENTRAL RESEARCH LIBRARY

CIRCULATION SECTION

4500N ROOM 175

LIBRARY LOAN COPY

DO NOT TRANSFER TO ANOTHER PERSON

If you wish someone else to see this
report, send in name with report and
the library will arrange a loan.

UCN-7969 (3-9-77)

Printed in the United States of America. Available from
National Technical Information Service
U.S. Department of Commerce
5285 Port Royal Road, Springfield, Virginia 22161
NTIS price codes—Printed Copy: A05 Microfiche A01

This report was prepared as an account of work sponsored by an agency of the United States Government. Neither the United States Government nor any agency thereof, nor any of their employees, makes any warranty, express or implied, or assumes any legal liability or responsibility for the accuracy, completeness, or usefulness of any information, apparatus, product, or process disclosed, or represents that its use would not infringe privately owned rights. Reference herein to any specific commercial product, process, or service by trade name, trademark, manufacturer, or otherwise, does not necessarily constitute or imply its endorsement, recommendation, or favoring by the United States Government or any agency thereof. The views and opinions of authors expressed herein do not necessarily state or reflect those of the United States Government or any agency thereof.

CHEMICAL TECHNOLOGY DIVISION

NUCLEAR WASTE PROGRAMS

ORNL Fixation of Waste in Concrete
(Activity No. AP 05 25 10 0, ONL-WHO2)

CEMENT-BASED RADIOACTIVE WASTE HOSTS FORMED UNDER ELEVATED
TEMPERATURES AND PRESSURES (FUETAP CONCRETES) FOR
SAVANNAH RIVER PLANT HIGH-LEVEL DEFENSE WASTE

L. R. Dole
G. C. Rogers
M. T. Morgan*
D. P. Stinton**
J. H. Kessler
S. M. Robinson
J. G. Moore*

*Retired.

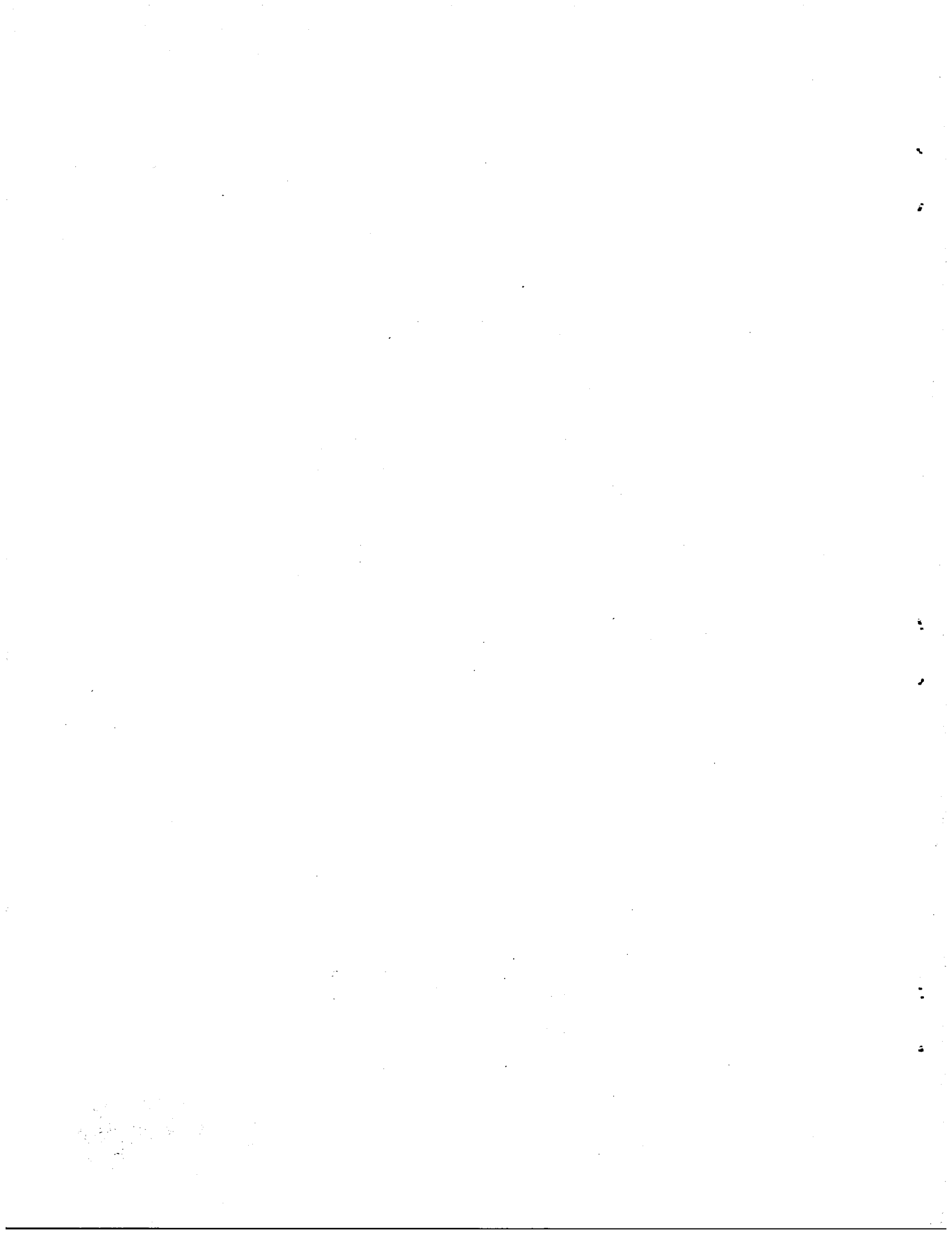
**Metals and Ceramics Division.

Date Published - March 1983

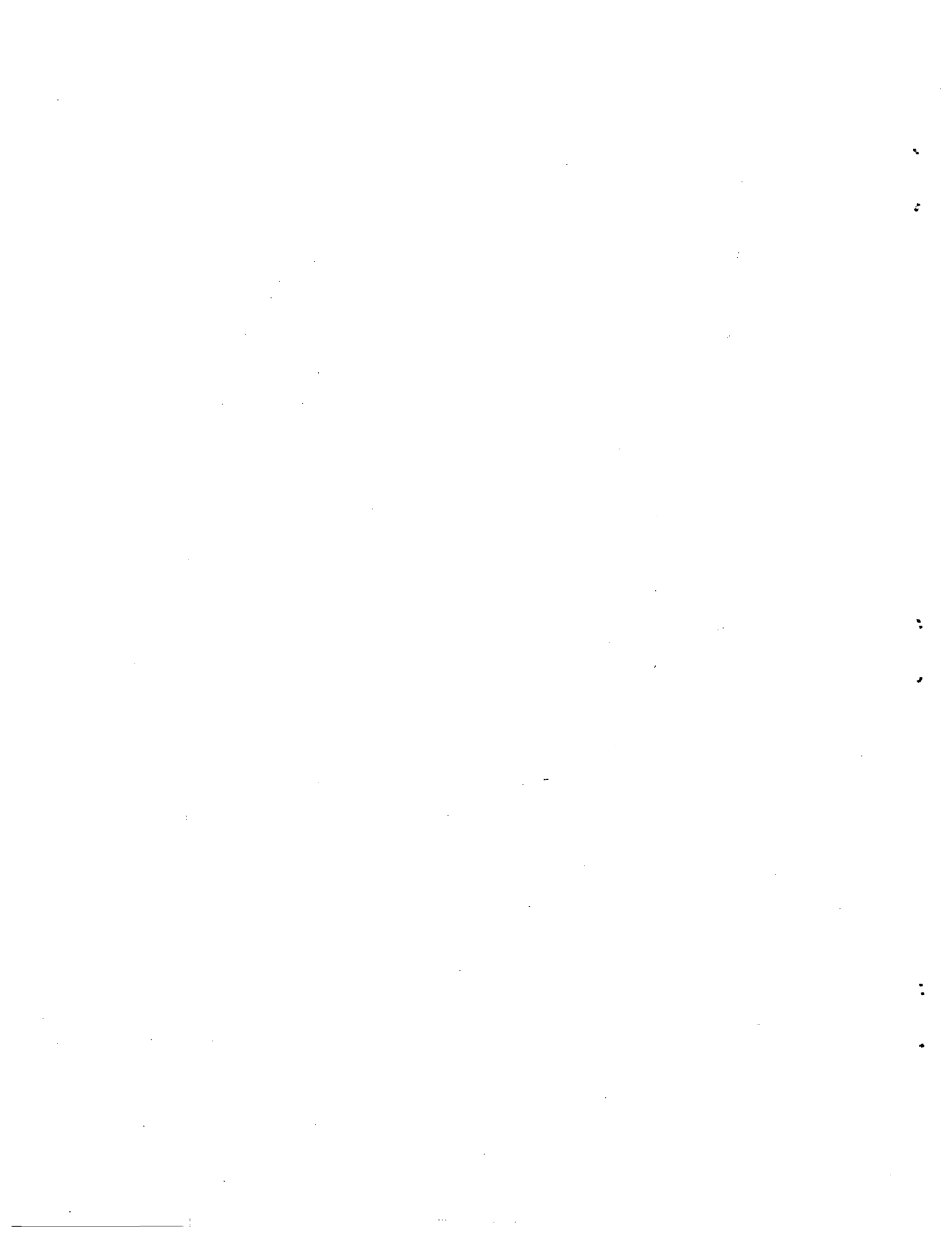
Prepared by the
OAK RIDGE NATIONAL LABORATORY
Oak Ridge, Tennessee 37830
operated by
UNION CARBIDE CORPORATION
for the
U.S. DEPARTMENT OF ENERGY
Under Contract No. W-7405-eng-26



3 4456 0251924 6



CONTENTS		<u>Page</u>
LIST OF TABLES		v
LIST OF FIGURES.		vii
ABSTRACT		1
1. INTRODUCTION		1
2. SAMPLE PREPARATION		3
2.1 COMPOSITION OF WASTE FORMS		4
2.2 PROCESSING OF SRP WASTES		7
2.3 EFFECTS OF WASTE COMPOSITION AND CURING CONDITIONS		12
3. PHYSICAL PROPERTIES		13
3.1 PERMEABILITY		14
3.2 POROSITY AND DENSITY		15
3.3 THERMAL CONDUCTIVITY		16
4. PHASE CHARACTERIZATION		25
5. LEACHABILITY		36
6. THERMAL STABILITY		47
7. RADIATION STABILITY		50
8. IMPACT STRENGTH		65
9. SUMMARY		67
10. REFERENCES		68
11. APPENDIXES		71



LIST OF TABLES

<u>Table</u>		<u>Page</u>
1	Reference composition of SRP waste solids	5
2	MCC-1 FUETAP mix for simulated SRP waste	6
3	Results of dewatering of the SRP FUETAP concretes	10
4	Minimum solids requirements for phase separation and set time for MCC-1 specimens	11
5	Effects of curing temperature and pressure on SRP FUETAP specimens	13
6	Typical properties of SRP FUETAP samples prepared with MCC-1 mix	14
7	Comparisons of physical properties of FUETAP mixes MCC-1 and MCC-2	18
8	Analysis of SRP FUETAP sample prepared with MCC-1 mix	26
9	SEM/EDX elemental analyses of phases in SRP FUETAP sample prepared with MCC-1 mix.	33
10	Possible phases found in MCC-1 FUETAP concrete containing SRP-4 waste	34
11	Typical values for the MCC-1 28-d leach rates from SRP FUETAP specimens in deionized water	37
12	Effects of Indian red pottery and bentonite clay additives on the leach rate of cesium from FUETAP concretes	39
13	Effect of cement type on MCC-1 28-d leach rates from FUETAP specimens in deionized water	39
14	Effect of temperature on leach rates from MCC-6A FUETAP specimens	41
15	Initial cesium release from SRP FUETAP specimens after 3-d leach with deionized water at 90°C	42
16	Results of FUETAP alpha-radiolysis tests with ²⁴⁴ Cm	52
17	Composition of gases generated in alpha-radiolysis tests of FUETAP concrete specimens	65

<u>Table</u>		<u>Page</u>
A.1	Compositions of SRP FUETAP concretes	74
A.2	Compositions of simulated SRP wastes	75
A.3	Physical properties of SRP FUETAP concretes	76
B.1	Duncan's multiple range test - uranium vs variable shown	78
B.2	Duncan's multiple range test for uranium concentration (ppm) vs temperature	79

LIST OF FIGURES

<u>Figure</u>		<u>Page</u>
1	Generalized FUETAP flowsheet for SRP waste	8
2	FUETAP flowsheet for Savannah River Plant site	9
3	Stack arrangement on thermal conductivity analyzer	17
4	Density of SRP FUETAP concretes as a function of water/cement ratio	19
5	Thermal conductivity of SRP FUETAP concretes as a function of water/cement ratio	20
6	Porosity of SRP FUETAP concretes as a function of water/cement ratio	21
7	Thermal conductivity of SRP FUETAP concretes as a function of sand concentration	22
8	Density of SRP FUETAP concrete as a function of sand concentration	23
9	Thermal conductivity of SRP FUETAP concretes as a function of density	24
10	MCC-1 concrete with Al _{kα} EDX spot analysis	28
11	MCC-1 concrete with Si _{kα} EDX spot analysis	29
12	MCC-1 concrete with Ca _{kα} EDX spot analysis	30
13	MCC-1 concrete with Fe _{kα} EDX spot analysis	31
14	Polished surface (SEM photograph) of MCC-1 SRP FUETAP concrete	32
15	Individual phases of hardened cement as a function of time	35
16	Strontium leach rates for three cements in four MCC-1 formulations using MCC-1 static leach test at 90°C with distilled water	40
17	MCC-1 strontium leach results at 90°C in deionized water for MCC-1 FUETAP concrete containing SRP-4 simulated waste	45

<u>Figure</u>		<u>Page</u>
18	Effects of clay additives on cesium leach rates from FUETAP concrete (MCC-1) in deionized water at 90°C . . .	46
19	Typical expansion curve of MCC-1 SRP FUETAP concrete specimens	49
20	Comparison of gas generation rates of SRP FUETAP concrete before and after dewatering (tests 1 through 3).	53
21	Alpha radiolysis of undewatered SRP FUETAP concrete containing 4.5 mg of ²⁴⁴ Cm in 8.2 g of host solid with gas sampling after 500 d (test 1)	55
22	Alpha radiolysis of duplicate dewatered SRP FUETAP concretes, each with 4.5 mg of ²⁴⁴ Cm in 8.2 g of host solid	57
23	Alpha radiolysis of a dewatered SRP FUETAP concrete with gas sampling after 500 d (test 2)	58
24	Superposition of the pressure rise after gas sampling (test 2).	59
25	Alpha radiolysis of duplicate dewatered SRP FUETAP concretes, each with 0.5 mg of ²⁴⁴ Cm in 8.2 g of host solid	60
26	Alpha radiolysis of a dewatered SRP FUETAP concrete containing 1.5 mg of ²⁴⁴ Cm in 8.2 g of host solid (test 6).	61
27	Comparison of gas generation rates of SRP FUETAP concrete before and after dewatering	63
28	Comparison of all gas generation rates of dewatered FUETAP concretes (tests 2 through 6).	64
29	Dynamic impact test of SRP FUETAP concrete specimens. . .	66

CEMENT-BASED RADIOACTIVE WASTE HOSTS FORMED UNDER ELEVATED
TEMPERATURES AND PRESSURES (FUETAP CONCRETES) FOR
SAVANNAH RIVER PLANT HIGH-LEVEL DEFENSE WASTE

L. R. Dole, G. C. Rogers, M. T. Morgan, D. P. Stinton,
J. H. Kessler, S. M. Robinson, and J. G. Moore

ABSTRACT

Concretes that are formed under elevated temperatures and pressures (called FUETAP) are effective hosts for high-level radioactive defense wastes. Tailored concretes developed at the Oak Ridge National Laboratory (ORNL) have been prepared from common Portland cements, fly ash, sand, clays, and waste products. These concretes are produced by accelerated curing under mild autoclave conditions (85 to 200°C, 0.1 to 1.5 MPa) for 24 h. The solids are subsequently dewatered (to remove unbound water) at 250°C for 24 h. The resulting products are strong (compressive strength, 40 to 100 MPa), leach resistant [plutonium leaches at the rate of 10 pg/(cm²·d)], and radiolytically stable, monolithic waste forms (total gas value = 0.005 molecule/100 eV).

This report summarizes the results of a 4-year FUETAP development program for Savannah River Plant (SRP) high-level defense wastes. It addresses the major questions concerning the performance of concretes as radioactive waste forms. These include leachability, radiation stability, thermal stability, thermal conductivity, impact strength, permeability, phase complexity, and effect of waste composition.

1. INTRODUCTION

The use of cement in radioactive waste management has been the subject of several studies.¹ Cement has also been widely utilized for the fixation of low- and intermediate-level radioactive wastes at power reactor plants for about three decades.² Cementitious grouts are applied routinely at ORNL in the Hydrofracture Process for the fixation

and permanent disposal of locally generated intermediate-level waste (ILW) solutions.³⁻⁵ In this process, liquid waste streams are neutralized and the concentrated supernate is blended with a specially tailored cementitious dry mix. The resulting grout is then forced underground by pressure into the Conasauga shale formation underlying the plant. The grout solidifies after a few hours, fixing the radioactivity and removing it from man's environment. Laboratory studies have demonstrated that the leachabilities of cesium, strontium, and plutonium from these grouts are of the same order as those obtained for borosilicate glass. The results suggest that specially tailored cement-based mixes should form acceptable hosts for a wide variety of radioactive wastes.

Subsequent laboratory studies confirmed that FUETAP concretes offer considerable promise as hosts for the disposal of defense wastes, transuranium (TRU) wastes, and commercial high-level wastes.⁶ Roy and Gouda,⁷ of Pennsylvania State University, produced cements with high strength and low porosity by using conditions of high temperature (150 to 250°C) and pressure [25,000 to 50,000 psi (172 to 344 MPa)] for 0.5 to 2 h. They demonstrated that accelerating the curing could result in superior cement properties. On this basis, an investigation was begun at ORNL to examine the potential of forming concretes under elevated, but less stringent, temperatures and pressures than the previous study. Also, concretes containing specific additives to fix the nuclides were studied, as in the cases of grouts in hydrofracture and ¹²⁹I fixation in barium iodate concretes.^{8,9} Moore and co-workers determined that only mild autoclave conditions are needed to accelerate the curing of

tailored cements. Results of various tests showed that treatment at a temperature of 100°C and a pressure of 0.1 MPa for 24 h was usually sufficient to cure FUETAP concretes at a rate within realistic radioactive waste processing requirements.^{6,10-13}

The FUETAP concretes prepared by accelerated curing under these mild autoclave conditions have been found to be effective hosts for transuranic and high-level defense and commercial radioactive wastes.¹⁰⁻¹⁶ Some specific examples of wastes which have made acceptable FUETAP products are Nuclear Fuel Services Plant wastes, Rocky Flats startup by-products, Slagging Pyrolysis Incinerator fly ash, Andco-Torrax municipal waste frit, and SRP defense wastes. This document summarizes the FUETAP development program at ORNL for SRP defense wastes. It discusses the processing, leachability, alpha radiolysis, phase characterization, thermal expansion, impact strength, and physical properties of SRP concretes and reports the status of FUETAP concretes as hosts for radioactive wastes.

2. SAMPLE PREPARATION

The initial FUETAP formulations were based on hydrofracture grout mixes and were modified both to accommodate particular waste stream chemistries and to reduce the water demand. Only pourable mixes, which required a small amount of vibration to fill molds uniformly and to remove entrained air, were selected for study. Specimens were cast in sizes ranging from 1 mL to 75 L for the evaluation of leaching, compressive strength, thermal conductivity, porosity, permeability, density, and dewatering kinetics.

2.1 COMPOSITION OF WASTE FORMS

FUETAP concretes are prepared from common Portland cements, fly ash, sand, clay, and waste materials. Each concrete mix is tailored for the specific waste stream by optimizing the waste loading and maintaining a pourable mix with a minimum amount of water. Choosing the appropriate cement type and additives ensures a pourable mix which cures rapidly to a dense, durable solid with low leachability. The SRP mixes were designed to accommodate simulated wastes based on an average composition of the actual SRP wastes (Table 1). Abnormally high amounts of cesium and strontium were added to the simulated waste solids in order to ensure sufficient concentrations to allow accurate analyses in nonradioactive leach studies. This level is 3 to 3.5 times the normal chemical concentration that would be found in SRP waste. Although SRP wastes contain a significant level of nonradioactive cesium, the additional cesium and strontium result in the final simulated, nonradioactive waste forms containing the equivalent of 600 to 700 Ci/L.

Several concrete formulations (see Appendix A) were used during the 4-year development program. The compositions of the simulated SRP wastes and the formulation numbers that will be referenced throughout this report are also listed in Appendix A. The final reference composition of waste solids used by SRP¹⁷ is presented in Table 1. The basic FUETAP mix used for the materials characterization studies is MCC-1* (see Table 2). The cement/fly-ash ratio in the mixes was adjusted to

*MCC-1 is used to identify both a Materials Characterization Center static leach test and a specific SRP FUETAP concrete formulation.

Table 1. Reference composition of SRP waste solids^a

Component	Fraction of total (wt %)
Fe ₂ O ₃	47.16
Al ₂ O ₃	9.24
MnO ₂	12.98
CeO ₂	2.13
Gd ₂ O ₃ ^b	2.13
CaO ^b	2.51
NiO	5.84
SiO ₂	1.12
Na ₂ O	6.63
Na ₂ SO ₄	1.21
SrO ^b	1.00
Zeolite ^c	8.05

^aMajor elements only.

^bModification of formulation in DP-1545 (by Stone et. al.) to allow for uranium substitution and incorporation of 1 wt % SrO as requested by MCC.

^cThe zeolite (Ionsiv IE-95) was loaded with cesium equivalent to a Cs₂O loading of 12.4 wt % so that the final waste solids would contain 1 wt % cesium.

Table 2. MCC-1 FUETAP mix for simulated SRP waste

Component	Fraction of total (wt %)
Type I Portland cement	22.0
Fly ash	11.0
SRP simulated waste solids	20.0
Sand	27.75
D-65 water reducer	1.25
Water	18.00

maximize the compressive strength of the resulting solid and to increase strontium retention. Data from other concrete work suggest that this ratio should also produce a more stable solid.¹⁰ Sand was added to improve the thermal conductivity and the strength of the concrete. The water reducer (D-65), a proprietary compound from the Dowell Division of Dow Chemical (Houston, Tex.), was used to minimize the amount of water required to maintain a pourable grout.

Clays are often added to prevent cesium migration⁶ and therefore reduce leach rates. In our study, the zeolite present in the simulated wastes was assumed to serve as a cesium retainer. The formulations were kept as simple as possible, and clays were generally not added; however, preliminary tests in which clays were added to the formulations indicated that they reduce the leach rates (Sect. 5). A set regulator was added when it was needed to ensure a pourable mix.

2.2 PROCESSING OF SRP WASTES

A major advantage of FUETAP as a radioactive waste disposal alternative is its ease of processing. As illustrated in Fig. 1, calcined solids are blended in a drum or canister with the cementitious mix and a minimum amount of water. The mix is then solidified by curing at 85 to 200°C and 0.1 to 1.5 MPa. To obtain samples cured at 100°C, molds are closed and brought to temperature via a 1.5-h heatup in an autoclave. The specimens are cured for 24 h, then removed from the autoclave, and cooled to room temperature. The solidified material is dewatered by heating at 250°C for up to 24 h in order to minimize gasification by long-term radiolysis or heat. Samples with volumes less than 4 L are removed from the mold before dewatering, but the 4- to 75-L specimens are dewatered with only one end exposed. The dewatering is accomplished in a 250°C oven with rough vacuum for 24 h. Laboratory-scale studies have shown that more than 80% of the total unbound water loss occurs in the first 6 h, and there is no apparent diffusion lag in the water release. This treatment removes all of the unbound and a small amount of the hydrated water, leaving a hard, ceramic-like solid containing ~2 wt % water (Table 3). Following the dewatering step, the canister (or drum) is simply capped and stored.

The generalized flowsheet was modified (Fig. 2) to meet requirements specified by the SRP process evaluation team on May 7, 1981. This new flowsheet requires that 2 t of dry solids be added to a full charge of water and set regulator in a ribbon mixer within 2 h. Prior to initial blending, the transfer boom would be set to transfer to an abort/recycle

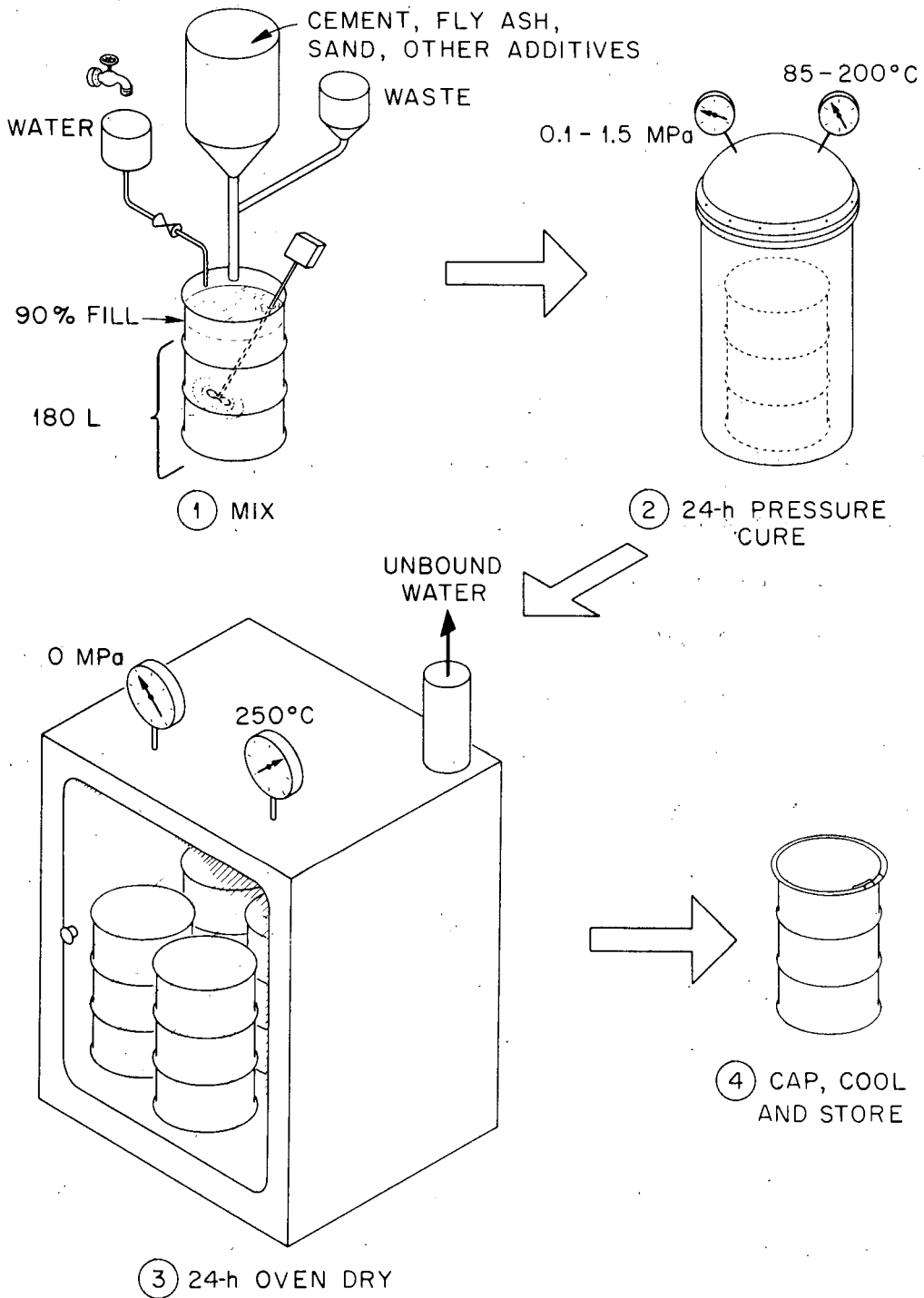


Fig. 1. Generalized FUETAP flowsheet for SRP waste.

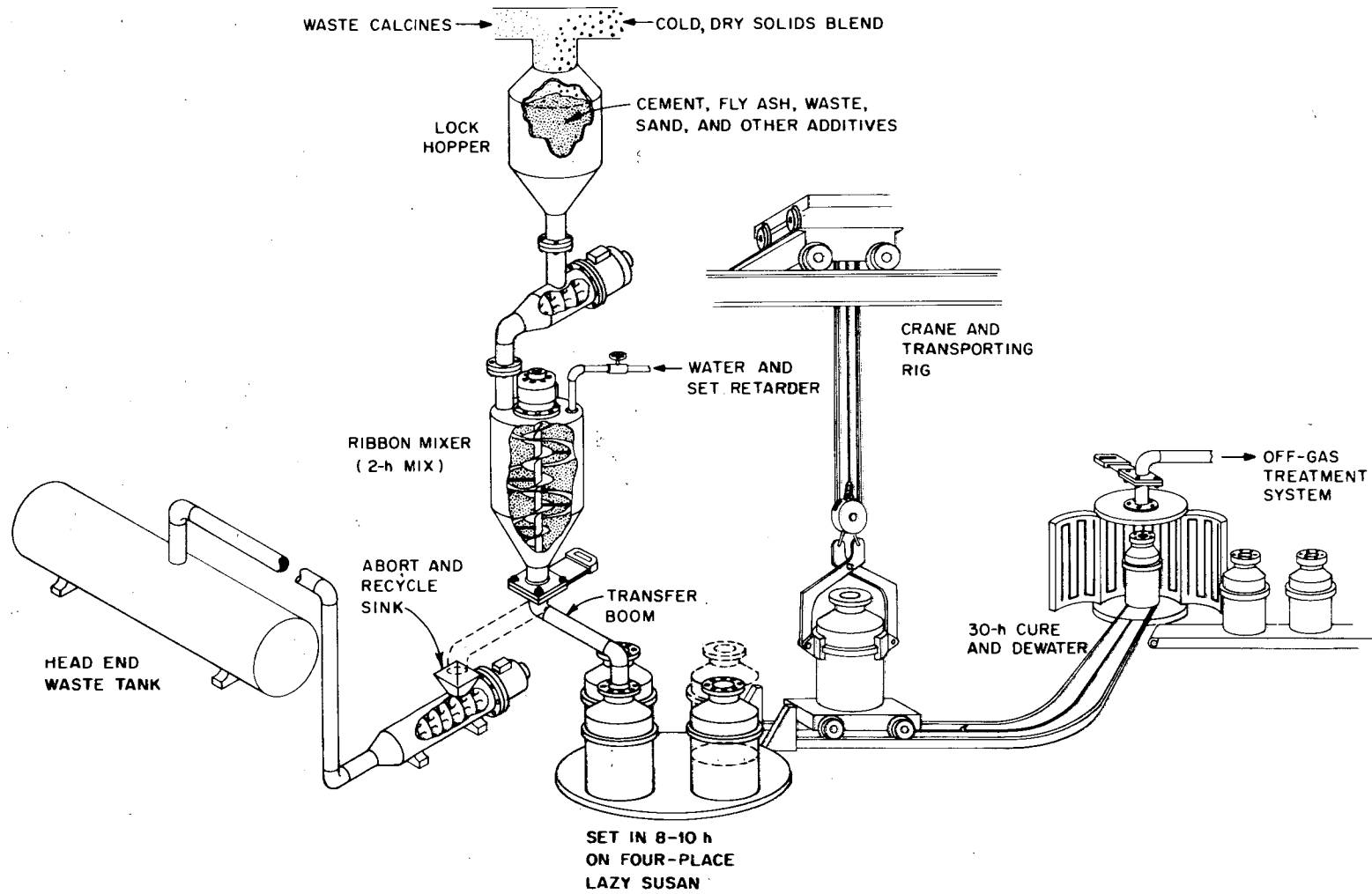


Fig. 2. FUE-TAP flowsheet for Savannah River Plant site.

Table 3. Results of dewatering the SRP FUETAP concretes

Temp. (°C)	Time (h)	Weight loss (%)	Volatiles lost ^a (%)	Water remaining (wt %) ^b
250	5	12.34	67	3.0
	24	13.08	71	2.2
	48	13.29	72	2.0 ^c
400	5	14.91	81	d
	24	15.08	82	d
900	24	16.97	92	d

^aInitial grout made up to contain 15 wt % H₂O. Other ingredients of the mix normally lose 3.41% of their total weight on heating 24 h at 900°C.

^bPercentages are approximate.

^cRepresents removal of all unbound water, as well as a small amount of hydrate-water.

^dMass spectrometry indicates that decomposition of hydrates, nitrates, and carbonates occurs at temperatures >400°C.

sink; however, after blending had proceeded to the point where an acceptable product could be made, the transfer boom would be moved to the normal position to discharge into canisters positioned on a four-place lazy Susan. Eight to ten hours after the canister had been filled, it would be transferred by cranes and a trolley to the curing-dewatering cell. Here the canister would be connected to a vacuum off-gas treatment manifold, and the connections would be tested for leaks. After the noncondensable gas had been removed, the vacuum off-gas system would be turned off and the concrete would be cured by heating the canister at 85 to 200°C for 12 to 16 h. Then, the vacuum off-gas system would be turned on and the temperature increased to 250°C for 14 to 18 h.

Laboratory tests have confirmed that curing and dewatering in 30 h will yield products with excellent mechanical properties.

Tests were made to assess the consequences of possible abnormal processing events, such as a broken blender shaft or a frozen transfer boom, in the proposed SRP flowsheet. Various amounts of simulated waste were added to a full charge of water, set regulator, and water reducer to determine the minimum amount of solids required for acceptable phase separation and set time. The results are shown in Table 4, where set time is defined as the time required for the mix to harden to such a degree that it will not flow from the container even under considerable impact force (e.g., if it was inverted and dropped from a crane). Phase separation occurs when free water collects on the surface as a result of

Table 4. Minimum solids requirements for phase separation and set time for MCC-1 specimens

Solids added (%)	Set time (h)	Phase separation ^a (%)	Volume of liquid (cm ³)	Volume of solids (cm ³)
25	0	43	117.0	155.0
37.5	0	31	91.0	200.0
50	0	14	56.0	340.0
62.5	0	<1	3.0	365.0
75	<10	0		399.0
87.5	4-10	0		412.0

^aFree water collects on the surface as a result of mix segregation or gel shrinkage.

mix segregation or gel shrinkage. These data show that no auxiliary agitation, backup transfer system, or extraordinary operational procedures are required to deal with many abnormal events.

2.3 EFFECTS OF WASTE COMPOSITION AND CURING CONDITIONS

The different chemical reactivities and compositions of the various wastes to be incorporated in concrete make changes in FUETAP formulations necessary in order to ensure a desirable product, as described in Sect. 2.1. Waste particle size affects the rheology and most of the physical properties of the FUETAP concretes, including final porosity, density, and thermal conductivity. Therefore, waste loading depends on the particle size of the waste solids. Increased waste loadings without the appropriate formulation changes will generally result in increased mix viscosity, poorer compressive strength, and lower thermal conductivity in the final product. However, all requirements for an acceptable product can be met by using the proper combination of additives.

Although major variations in the waste composition have a profound influence on the mix formulation and the physical properties of the final product, minor variations appear to have little effect. This observation, noted by Moore et al. in 1971,⁶ is confirmed by data presented in Sect. 3. The physical properties of the FUETAP concretes made from various SRP wastes (Appendix A) are consistent and follow noticeable trends with changes in mix compositions.

Above threshold values, the physical properties appear to be independent of curing temperature and pressure. Mixes containing simulated

SRP waste yielded solids with essentially the same physical characteristics when cured for 24 h at temperatures from 100 to 250°C and pressures from 0.1 to 4.1 MPa (Table 5). Since the SRP wastes have only moderate radioactivity levels, the concretes containing these wastes are expected to exhibit little or no self-heating. Therefore, samples were usually cured at the lower temperature and pressure (100°C at 0.1 MPa), which would be the most extreme hydrothermal conditions expected in a repository.

Table 5. Effects of curing temperature and pressure on SRP FUETAP specimens

Temp. (°C)	Pressure (MPa)	Compressive strength (MPa)	Thermal conductivity [W/(m·K)]
100	0.1	61	-
100	0.6	62	1.00
160	0.6	54	1.00
250	4.1	58	1.05

3. PHYSICAL PROPERTIES

Laboratory-scale studies with simulated SRP waste show that the resulting FUETAP concretes have excellent properties and can be classified as high-strength concretes. Results of the tests on various FUETAP concretes are detailed in Appendix A and a supplement¹⁸ to this report; only a brief summary is given here. Typical values for concretes containing 20 wt % simulated SRP waste (MCC-1 formulation) are shown in Table 6. The compressive strength ranges from 60 to 100 MPa for samples

Table 6. Typical properties of SRP FUETAP samples prepared with MCC-1 mix

Physical property	Value
Density, g/cm ³	2
Compressive strength, MPa	60-100
Thermal conductivity, [W/(m·K)]	1
Porosity, %	22-26
Permeability, darcy	6×10^{-5}

dewatered for 24 h at 250°C. The thermal conductivity is 1 W/(m·K); the density is 2 g/cm³, and the porosity ranges from 22 to 26%. The permeability is only $\sim 6 \times 10^{-5}$ darcy ($\sim 6 \times 10^{-17}$ m²), a fairly typical value for a normal dewatered concrete.

3.1 PERMEABILITY

The permeabilities of the FUETAP concretes were determined from dewatered samples. Nitrogen gas was used as the working fluid, and flow rates were measured at three different pressures; then Darcy's law was applied to calculate the apparent permeability. The permeability to a selected fluid was determined by applying the Klinkenberg correction to the three apparent permeability determinations. That is, the log of the permeability was plotted as a function of the reciprocal of the pressure differential, and the linear relationship was then extrapolated to infinite pressure. (At this intercept, the apparent permeability equals the permeability to any fluid.) Results showed that the permeability varied with the formulation and waste particle size, ranging from 1.0×10^{-6} to

1.0×10^{-3} darcy for most FUETAP concretes, and was directly proportional to the water/cement ratio.

3.2 POROSITY AND DENSITY

Porosities and densities were usually measured by immersing the vacuum-dried samples in toluene (25 mL); however, a few mercury intrusion measurements were made. In the toluene immersion tests, samples were cut and ground to right-circular cylinders. Measurements were made at multiple positions to determine precision of shape and to obtain average dimensions. Samples were then dried for at least 16 h in a vacuum oven [~ 30 in. Hg (~ 20 Pa)] at 100°C , cooled in bottles containing a desiccant, and then weighed. From these measurements, values were obtained for the cylinder's geometric volume [V_{geo} (cm^3)], dry weight [W_{dry} (g)], and density [ρ (g/cm^3)]. Samples were evacuated at ~ 30 in. Hg (~ 20 Pa) for 1 h and then submerged in toluene for at least 8 h in order to achieve saturation. Following this treatment, the samples were weighed, still submerged, to obtain W_{sub} . By Archimedes' principle, the volume of the solid, as determined by its liquid displacement, is $V_s = (W_{\text{dry}} - W_{\text{sub}})/\rho_t$, where ρ_t is the density of toluene. Porosity is calculated by:

$$P = \frac{V_{\text{geo}} - V_s}{V_{\text{geo}}}, \text{ or } P (\%) = 100 \left[1 - \frac{W_{\text{dry}} - W_{\text{sub}}}{\rho_t V_{\text{geo}}} \right].$$

The density of the concrete sample fully saturated with water is calculated as follows: $\rho_{\text{sat}} = (W_{\text{dry}} + P V_{\text{geo}} \rho_{\text{water}})/V_{\text{geo}}$, and the density of the solid (approximately theoretical) can be determined from:

$$\rho_s = W_{\text{dry}}/V_s = (W_{\text{dry}}\rho_t)/(W_{\text{dry}} - W_{\text{sub}}). \text{ The greatest sources of error}$$

were in the drying and saturation procedures. Dimensions were reproducible to 0.1 mm, or ~1%, while weights were accurate to >0.03%. Assuming that drying and saturation were carried to >95% completion, the overall estimated error was <2% in V , ρ , and W but might be >30% in P .

3.3 THERMAL CONDUCTIVITY

A Dynatech TCFCM-20 comparative, thermal conductivity analyzer was used to measure the thermal conductivities of the cementitious solids.¹⁹ In this instrument a short, right-circular cylinder 2 in. OD and 0.5 to 1.0 in. high (5.1 cm OD x 1.3-2.5 cm high) is sandwiched between two Pyrex 7740 reference disks of the same diameter (Fig. 3). Heat flows from the main heater at the top of the stack to the heat sink at the bottom. A second heater is used to control the temperature at the bottom. Metal spacers are placed between the heaters and the reference disks to equalize the heat flux over the horizontal cross section of the stack. A guard ring surrounding the stack is maintained at the same temperature gradient as that existing in the stack to prevent radial heat loss.

Temperatures are measured either by thermocouples embedded in grooves in the interface surfaces of the samples and reference materials or by temperature-sensing disks. The latter are thin, circular plates of nickel into which a radial hole has been drilled for insertion of a thermocouple. Although the former technique is more accurate, the attendant sample preparation is quite time-consuming; thus, the temperature-sensing disks are used for most screening measurements.

ORNL DWG 79-242R2

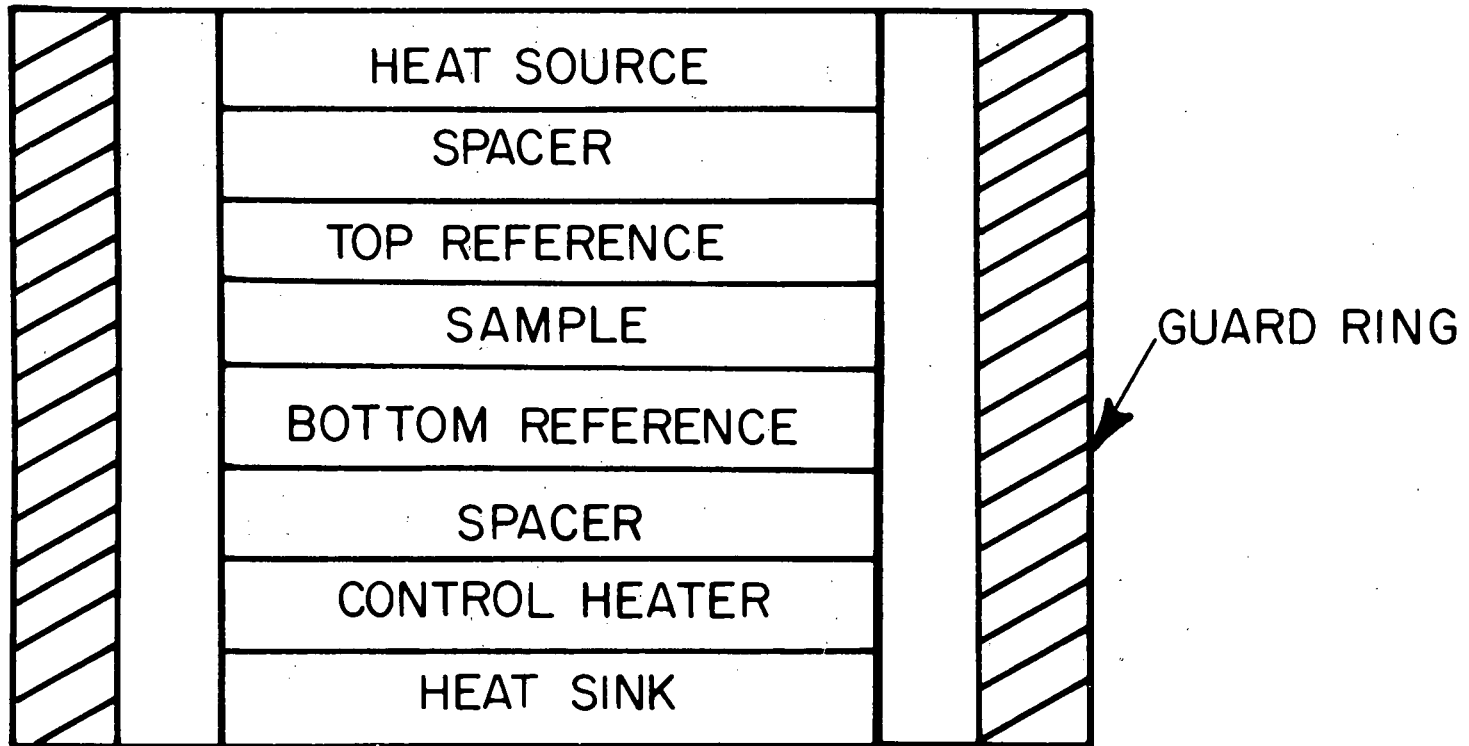


Fig. 3. Stack arrangement on thermal conductivity analyzer.

After the required temperatures have been measured, thermal conductivities are calculated from the equation:

$$k_s = \frac{X_s}{2\Delta T_s} \left(\frac{k_t \Delta T_t}{X_t} + \frac{k_b \Delta T_b}{X_b} \right),$$

where

k = thermal conductivity, $W/(m \cdot K)$;

ΔT = temperature differential, K ;

X = thickness, cm ;

s, t, b = subscripts referring to the sample, top reference, and bottom reference materials in the test stack, respectively.

Although this equation is only applicable in cases where the interface areas are equal and there is no radial heat flow, experimental results show that variations in area of <12% would change the results by <3%.

Table 7 compares FUETAP concretes prepared from mixes MCC-1 and MCC-2. These data show the advantages of minimizing the water/cement ratio. The lower limit of this ratio is determined by the processibility or workability of the mix. Figures 4 through 9 show trends in the

Table 7. Comparisons of physical properties of FUETAP mixes MCC-1 and MCC-2

FUETAP mix	Porosity (%)	Dry bulk density (g/cm^3)	Thermal conductivity [$W/(m \cdot K)$]	Water/cement ratio
MCC-1	29.5	1.91	0.90	0.81
MCC-2	26.9	1.94	0.95	0.75

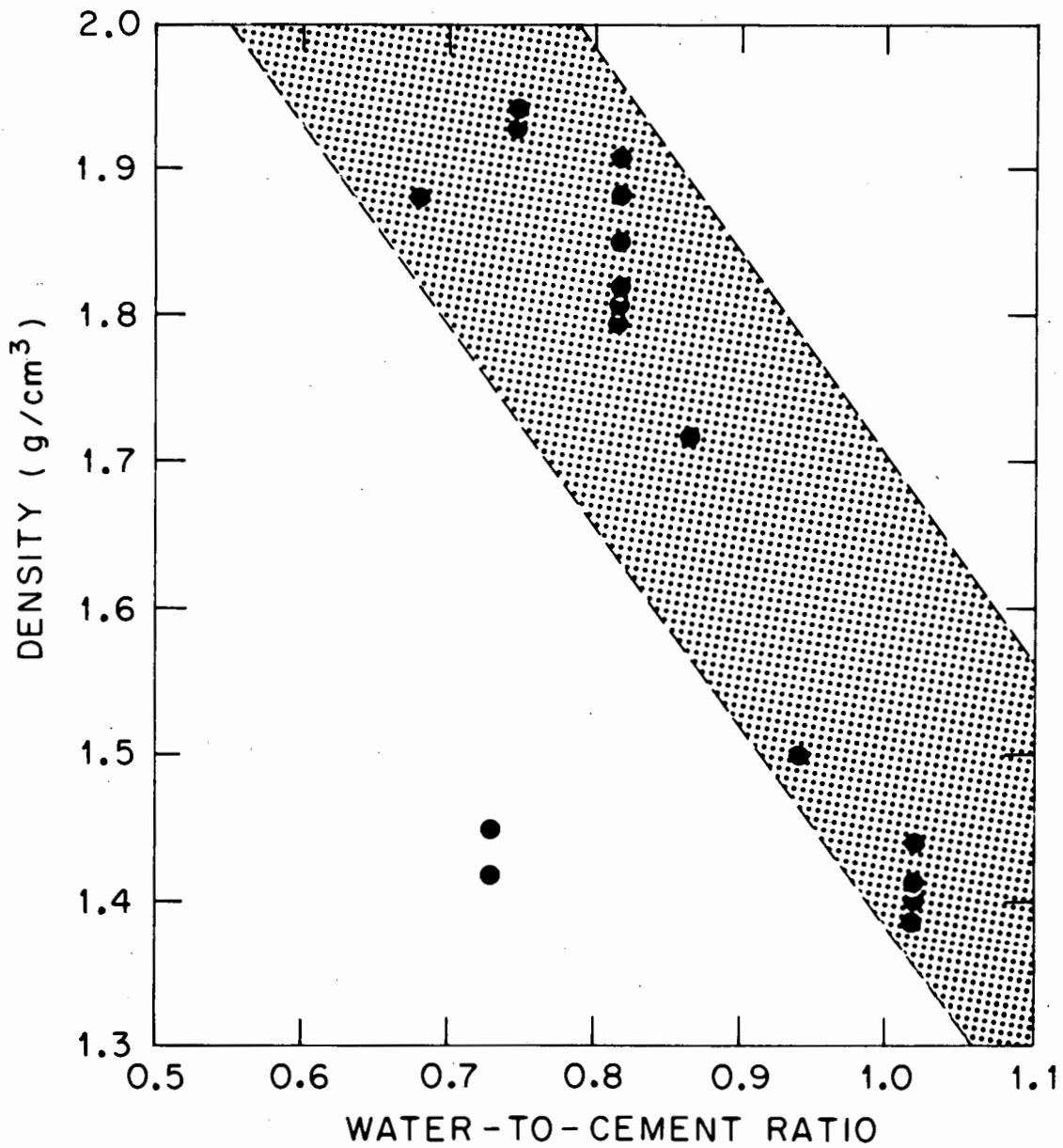


Fig. 4. Density of SRP FUEATAP concretes as a function of water/cement ratio.

ORNL DWG 83-193

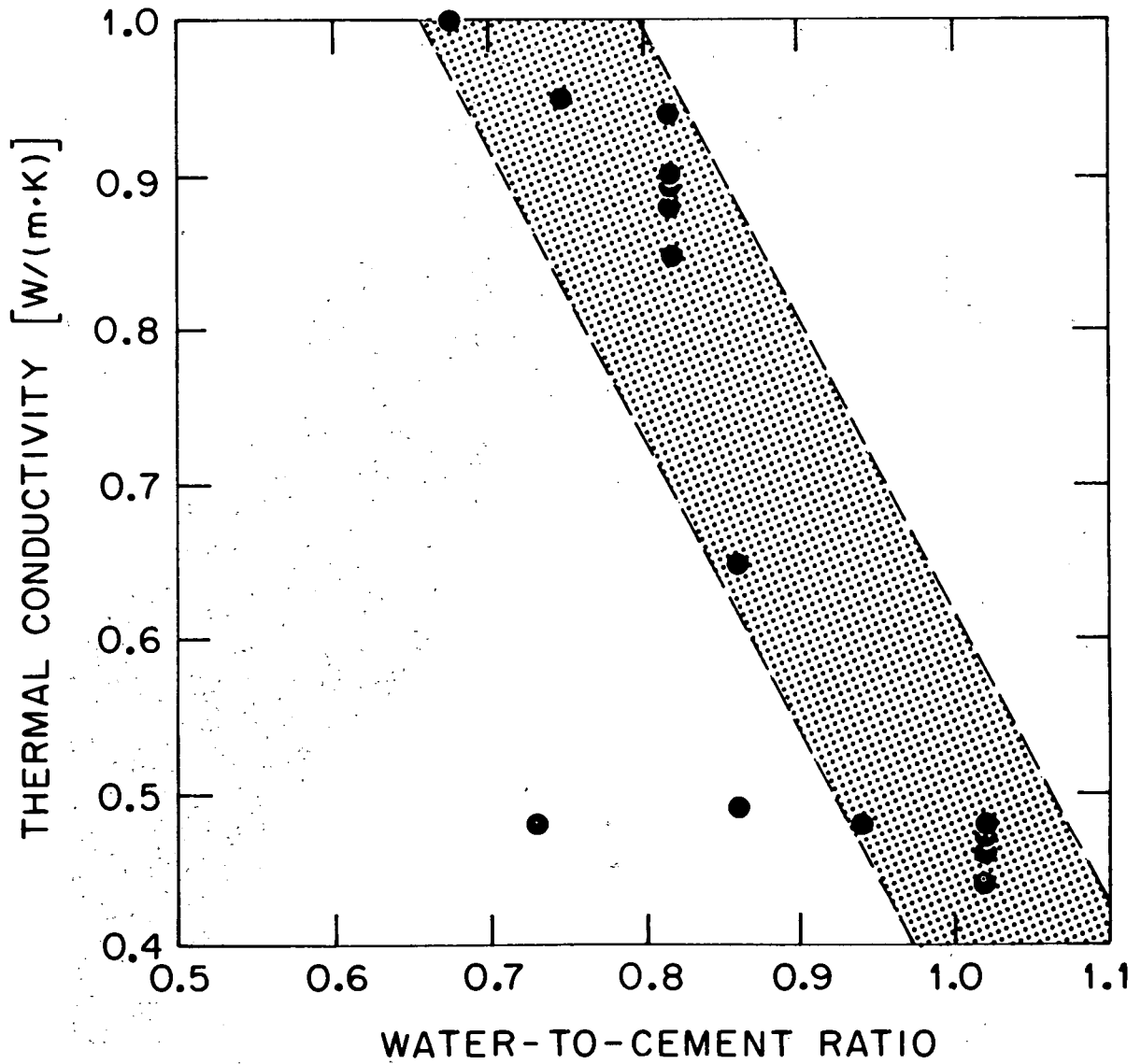


Fig. 5. Thermal conductivity of SRP FUETAP concretes as a function of water/cement ratio.

ORNL DWG 83-191

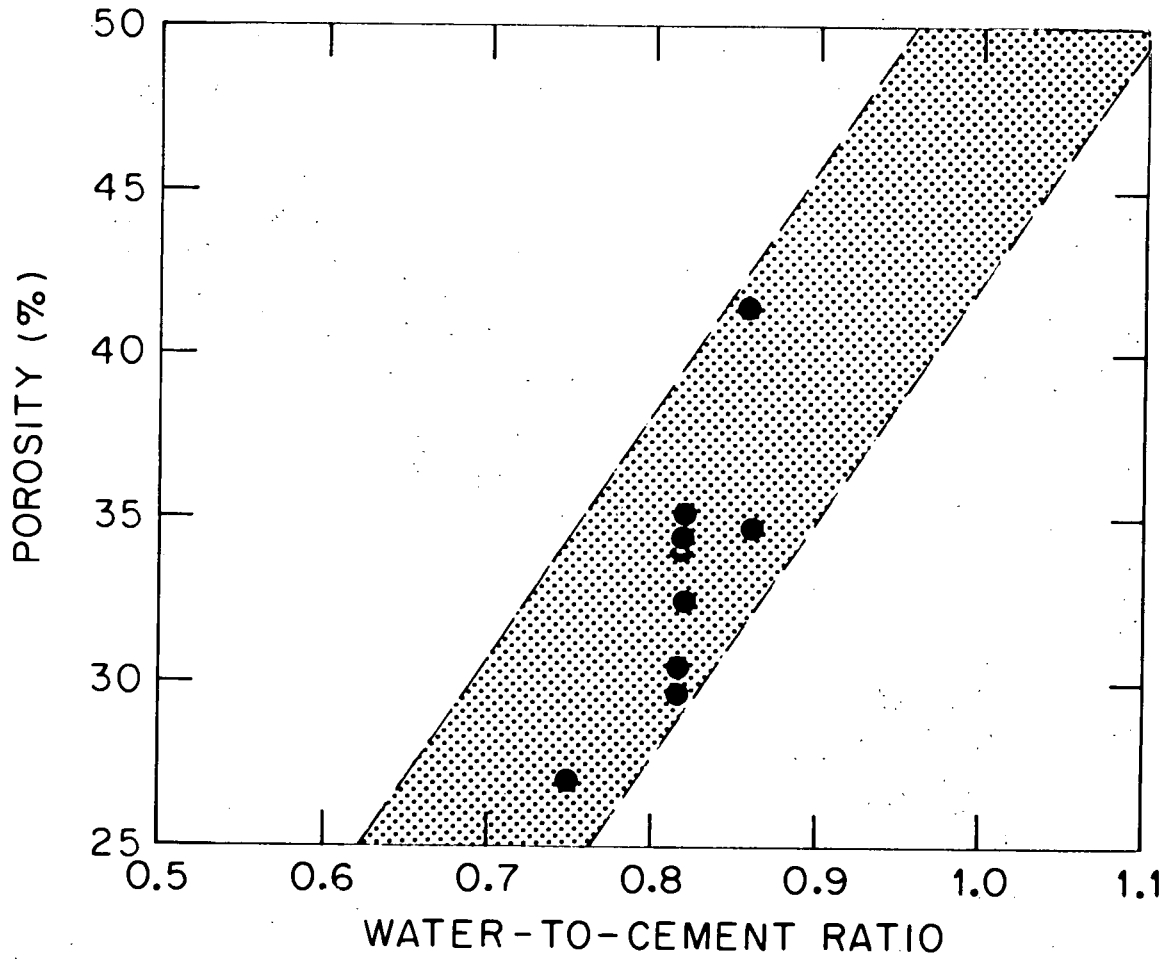


Fig. 6. Porosity of SRP FUETAP concretes as a function of water/cement ratio.

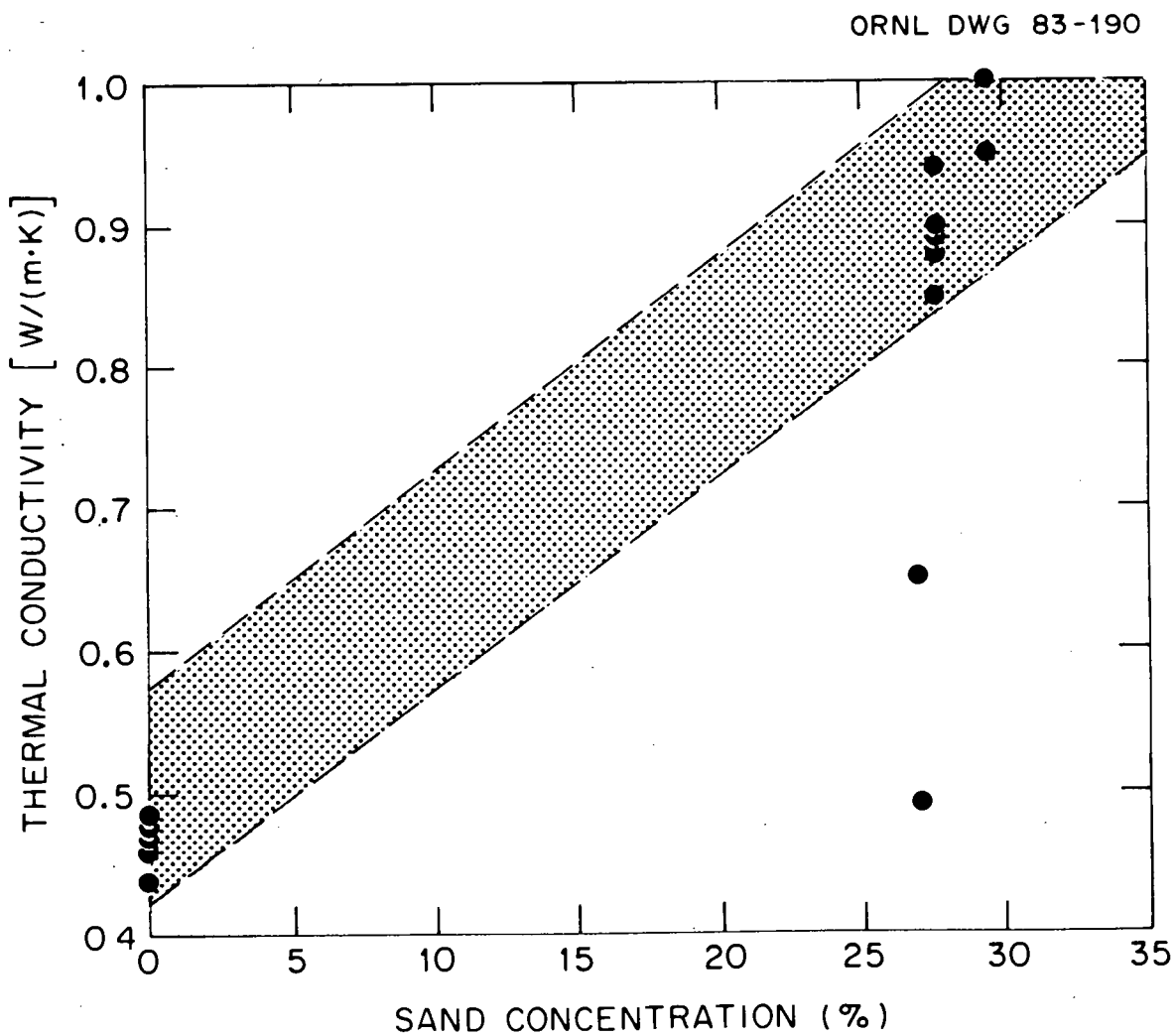


Fig. 7. Thermal conductivity of SRP FUEAP concretes as a function of sand concentration.

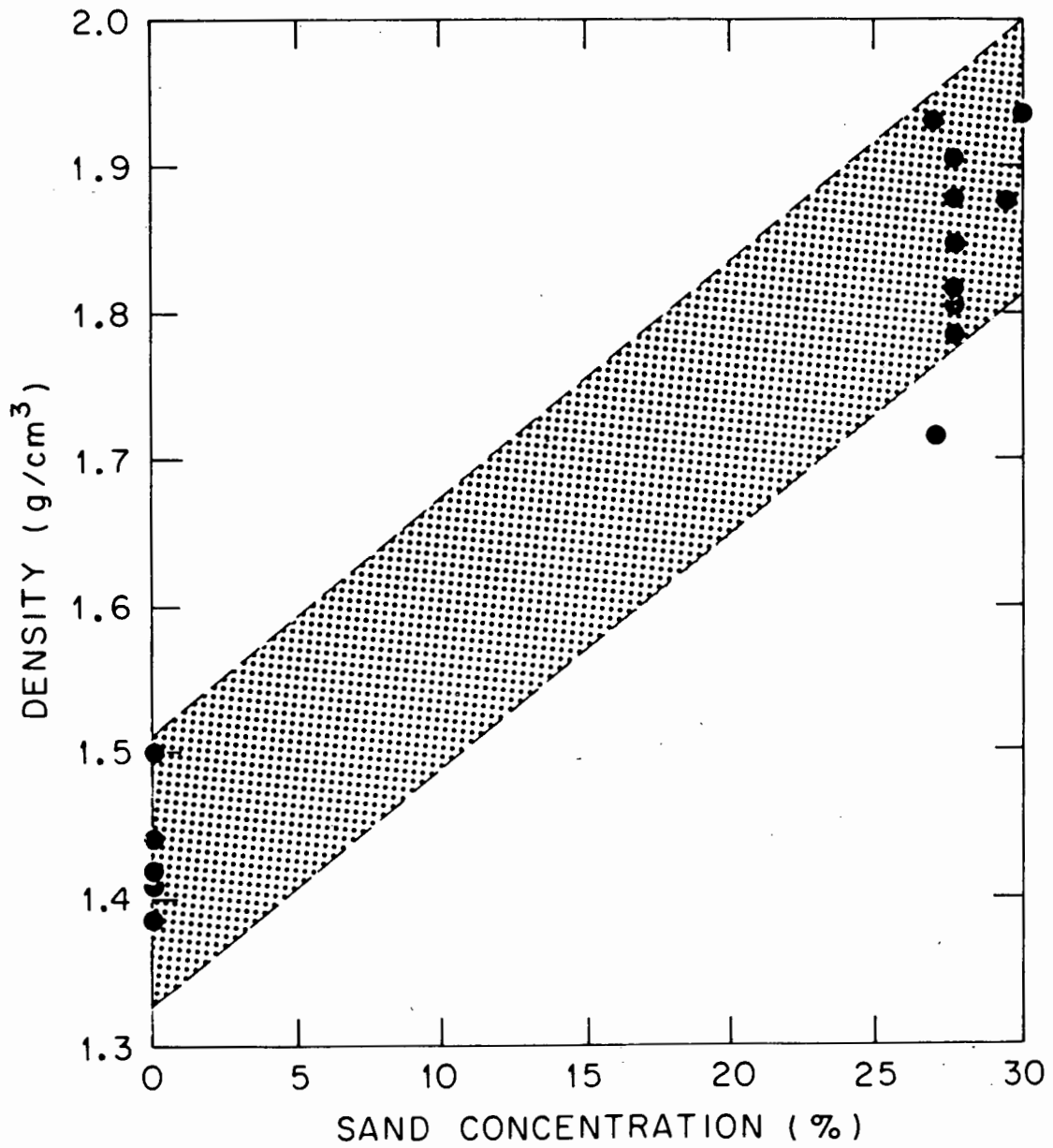


Fig. 8. Density of SRP FUEAP concrete as a function of sand concentration.

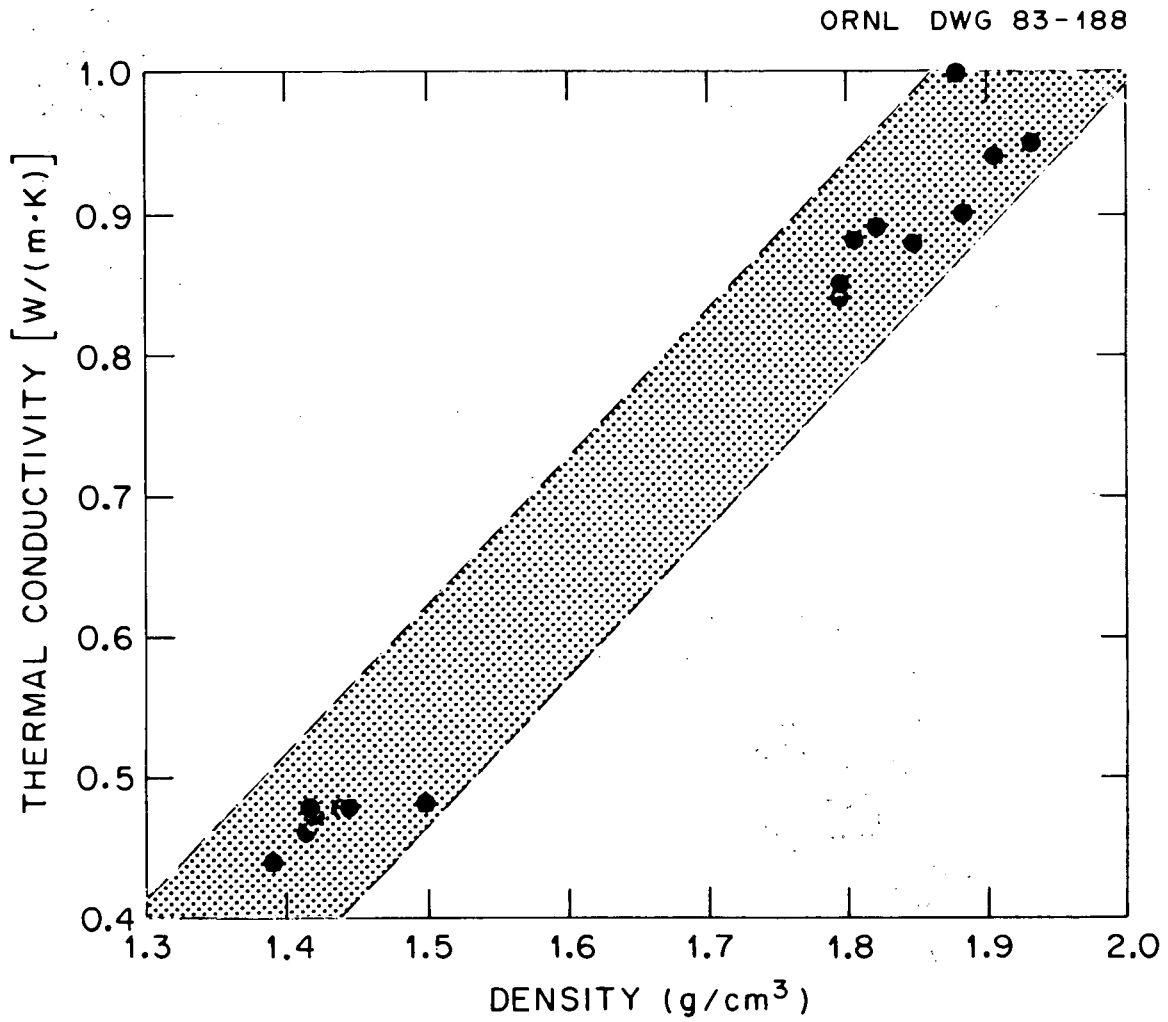


Fig. 9. Thermal conductivity of SRP FUETAP concretes as a function of density.

physical properties of SRP concretes. The data points tend to be scattered because the concretes contained a variety of SRP waste solids and waste formulations which affected the physical properties (Sect. 2.3). Although direct correlations cannot be made from these results, the general trends follow those of FUETAP concretes containing other wastes on which more detailed studies have been made. The density and the thermal conductivity decrease with increasing water/cement ratios, while the porosity increases. Both the thermal conductivity and the density increase with sand concentration, which was kept below 30 wt % since larger amounts reduce the compressive strengths. The thermal conductivity is directly proportional to the density.

4. PHASE CHARACTERIZATION

The ordinary, wet-method analytical results for a solidified FUETAP concrete (MCC-1) containing 20% simulated waste are shown in Table 8. Silicon was volatilized while the sample was being prepared for analysis (due to fluoride dissolution) and therefore is not included in the list.

In a series of preliminary studies made by the Metals and Ceramics Division of ORNL, the individual phases of SRP FUETAP concrete specimens were examined and characterized using optical microscopy, scanning electron microscopy (SEM), and electron microprobe analysis. Both fracture surfaces and polished sections of MCC-1 FUETAP samples (1.5 cm diam) were examined in an attempt to characterize the materials. Samples for SEM or microprobe study were mounted in epoxy, carefully polished, and coated with a conductive layer of carbon or gold prior to examination.

Table 8. Analysis of SRP FUETAP sample prepared with MCC-1 mix^a

Element	Fraction of total (wt %)
Al	2.56
Ba	0.02
Ca	11.29
Ce	0.34
Co	0.01
Cr	0.01
Cs	0.13 ^b
Fe	8.22
Gd	0.04
K	0.23
La	0.01
Mg	0.44
Mn	1.79
Na	0.87
Ni	0.91
P	0.03
Sr	0.22 ^c
Ti	0.13

^aSilicon was volatilized during sample preparation.

^bCesium value is low because of sodium interference.

^cStrontium value includes the amount present in the cement and fly ash.

Numerous phases were observed when a specimen was examined under an optical microscope using polarized light. The largest phase (500 to 1000 μm) was silica from the included sand. Small red phases (50 to 300 μm), probably Fe_2O_3 , were scattered throughout the field of view. A few metallic inclusions (50 to 150 μm) were also seen and were later confirmed as nickel by microprobe studies.

An energy dispersive x-ray analyzer (EDX) was used in conjunction with a SEM which used backscattered electrons to reveal the locations of calcium, silicon, aluminum, and iron on the surfaces of MCC-1 samples. Calcium, silicon, and aluminum were evenly distributed over the surfaces, except for one large sand grain (SiO_2) and many smaller scattered phases of mostly iron oxides (Figs. 10 through 13). The concerned elements are shown as light areas in the top photograph (SEM) of these figures. As many as nine or ten phases have been detected by using the SEM in conjunction with the EDX counting system. A SEM photograph and results of EDX analysis of a typical sample are found in Fig. 14 and Table 9, respectively.

At present, we can only make guesses concerning the identity of the phases in the SRP FUETAP concrete. Preliminary analyses have confirmed the presence of grains of quartz (sand), Fe_2O_3 , zeolite, Gd_2O_3 , and calcium aluminum hydrate. Manganese and nickel were also present in discrete grains that were deficient in other major components (Table 10). The discovery that both cesium and strontium are present in discrete phases has been of major importance in these studies. Cesium is located either in the zeolite or in a cement phase with high silicon and aluminum concentrations. Strontium has only been found in a phase rich in manganese.

It is extremely difficult to identify individual cement phases within a hardened FUETAP sample because the phases of cement grow together as they hydrate. After samples are cured at room temperature for 3 to 6 months, the phases are so intergrown that no single-phase

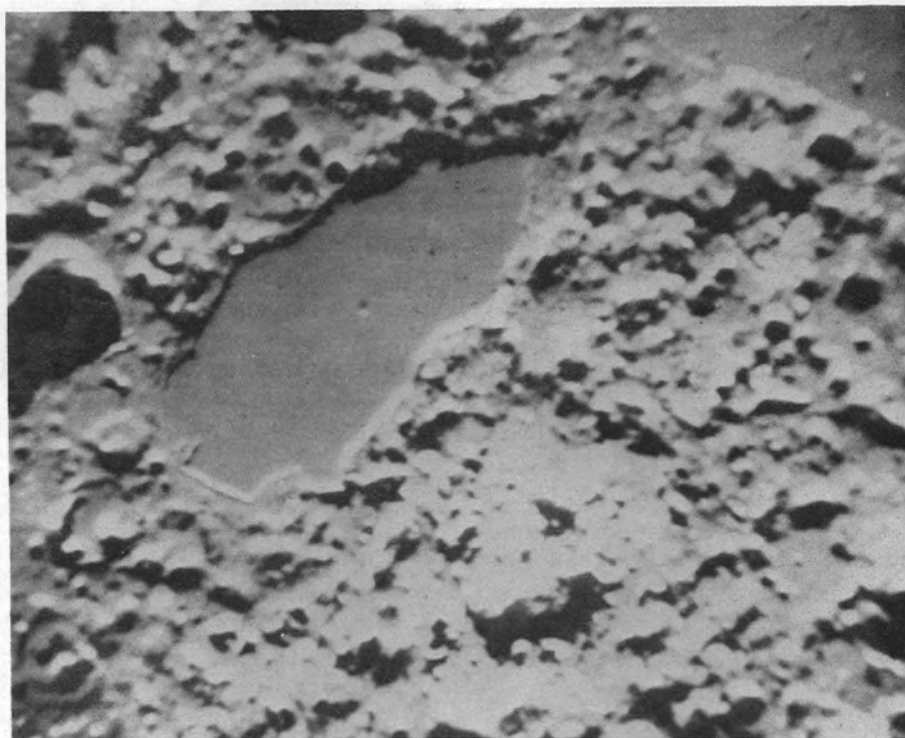
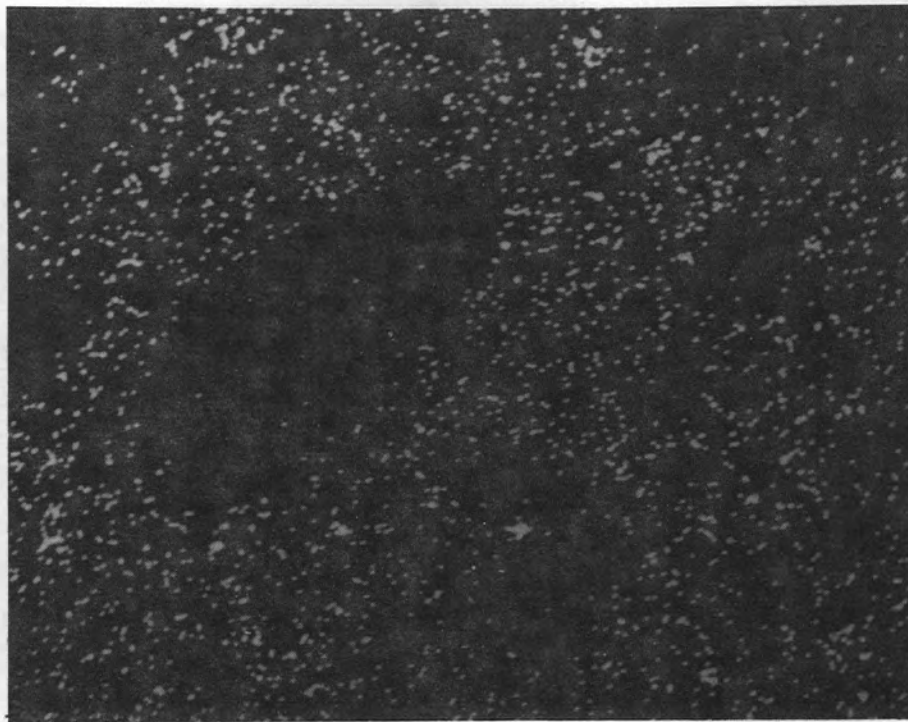


Fig. 10. MCC-1 concrete with $Al_{k\alpha}$ EDX spot analysis.

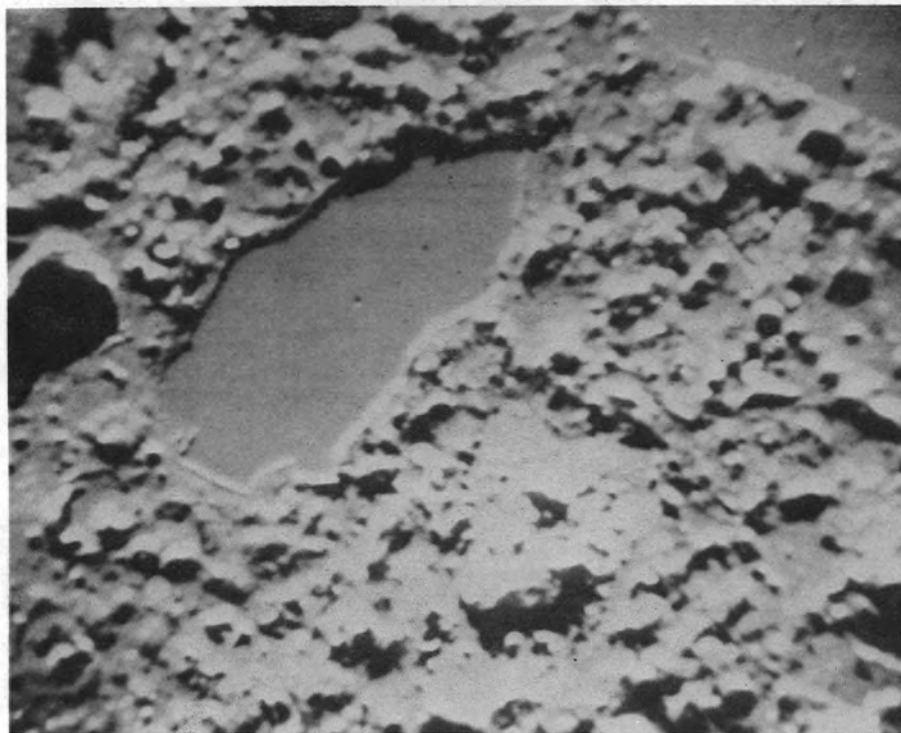
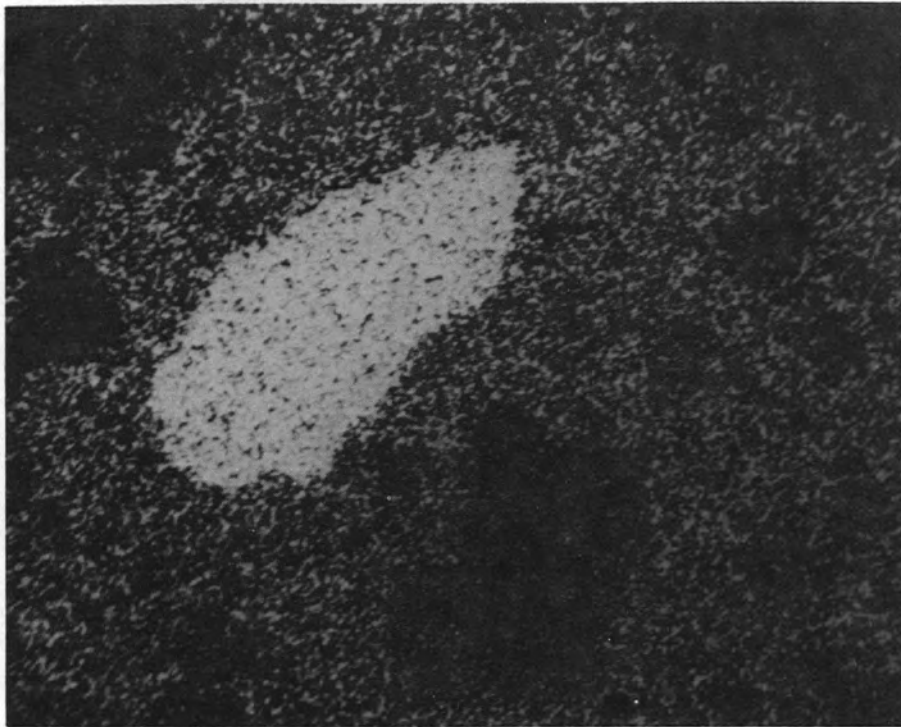


Fig. 11. MCC-1 concrete with $\text{Si}_{k\alpha}$ EDX spot analysis.

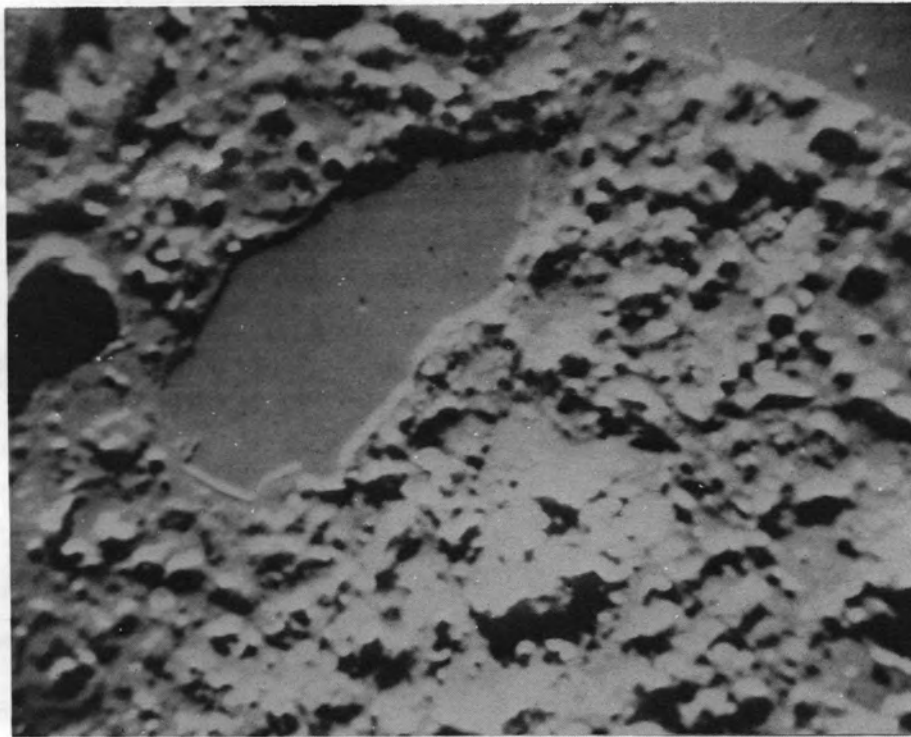
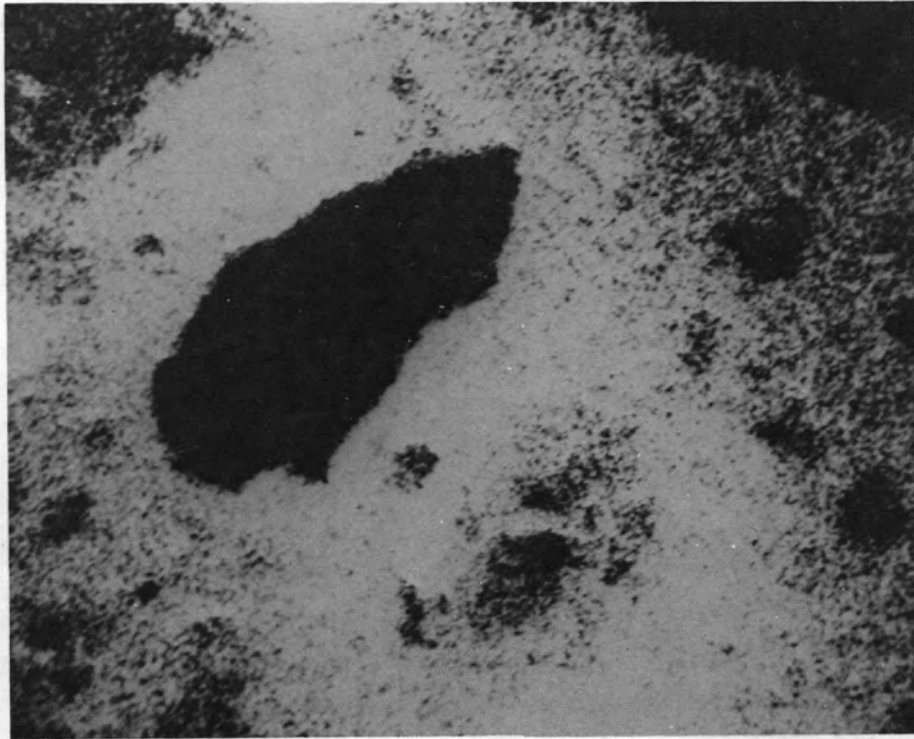


Fig. 12. MCC-1 concrete with $\text{Ca}_{k\alpha}$ EDX spot analysis.

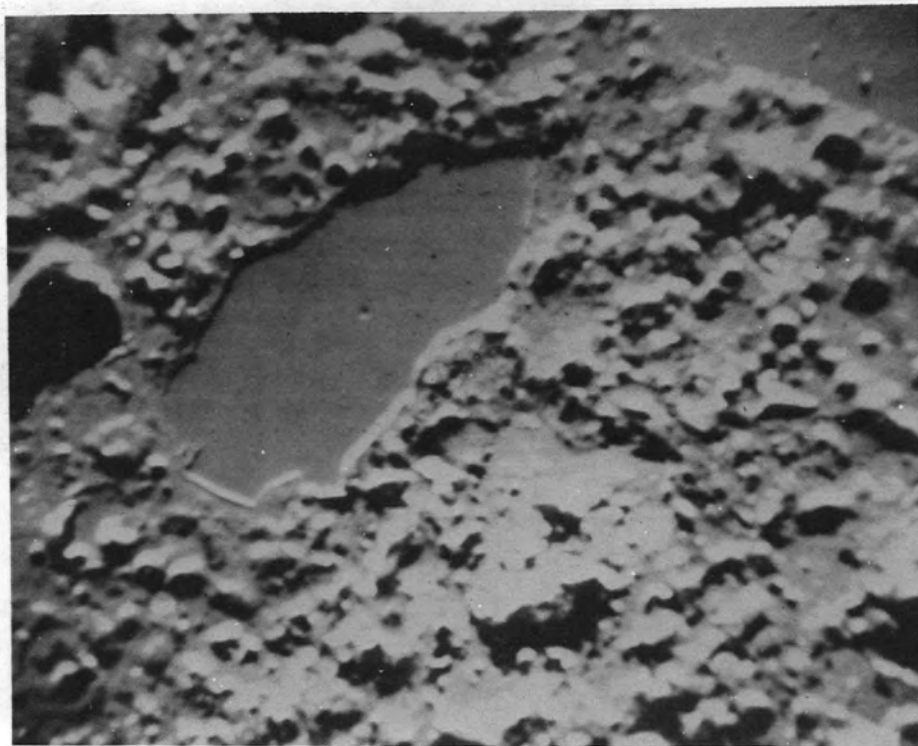
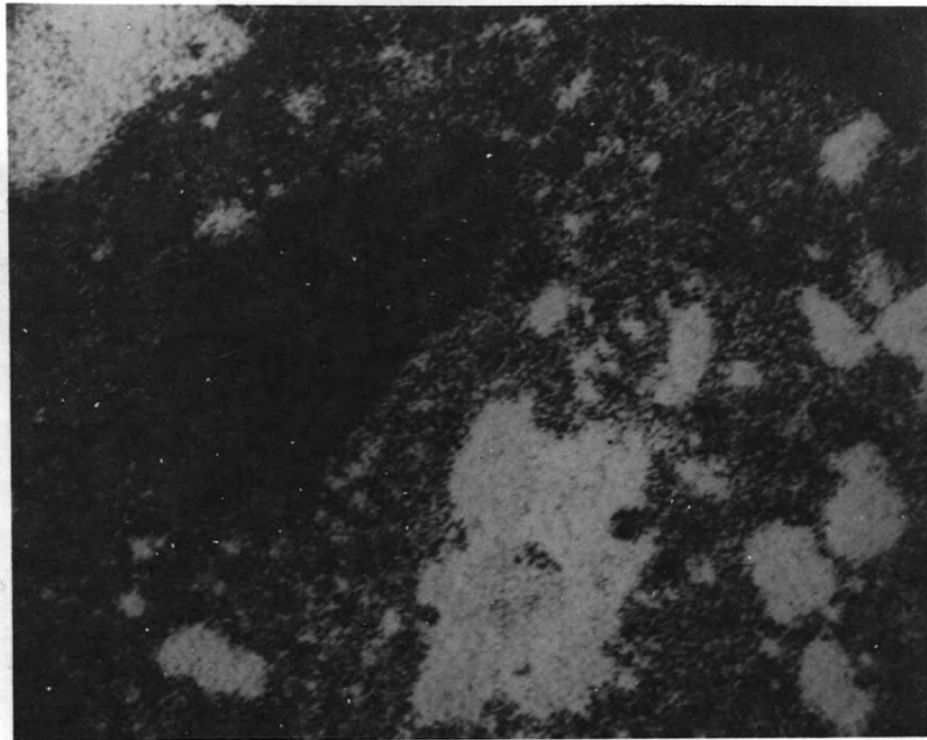


Fig. 13. MCC-1 concrete with $Fe_{k\alpha}$ EDX spot analysis.

ORNL-DWG 81-15677R

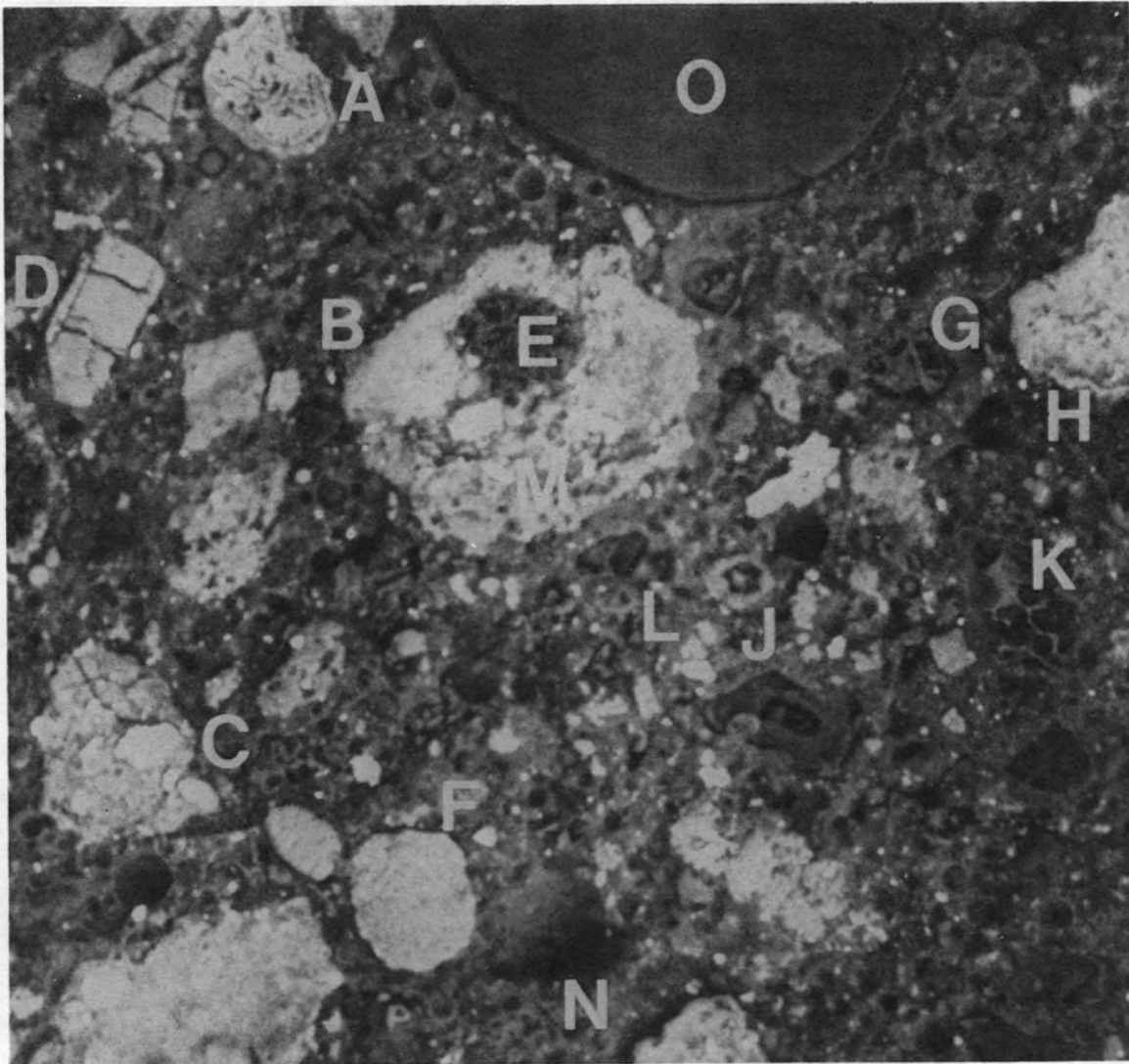


Fig. 14. Polished surface (SEM photograph) of MCC-1 SRP FUETAP concrete.

Table 9. SEM/EDX elemental analyses of phases in SRP FUETAP
sample prepared with MCC-1 mix

Phase	Elements	
	Major	Minor
A	Ni	Ca, Si, Al, S, Fe
B	Fe	Ca
C	Gd	Ca, Co, Si, Cr(?), Al
D	Mn	Ca, Si, K, Cr(?), Sr
E	Al	Ca, Fe
F	Fe	Ca, Si, Al, S, K
G	Ca	Si, Al, Fe, S, Mg, K(?), Ti
H	Fe, Ca, Si, Al	Ni, Mn, S
J	Si, Ca, Al	Cs, S, Na, K, Fe
K	Ca, Si, Al	Fe, Mg, S, Ti
L	Ca, Si, Al, Fe	S, K, Ti(?)
M	Fe, Ca	Si, S, Al
N	Ca, Si, Al, Fe	Ti, K, S, Mn, Na
O	Si	

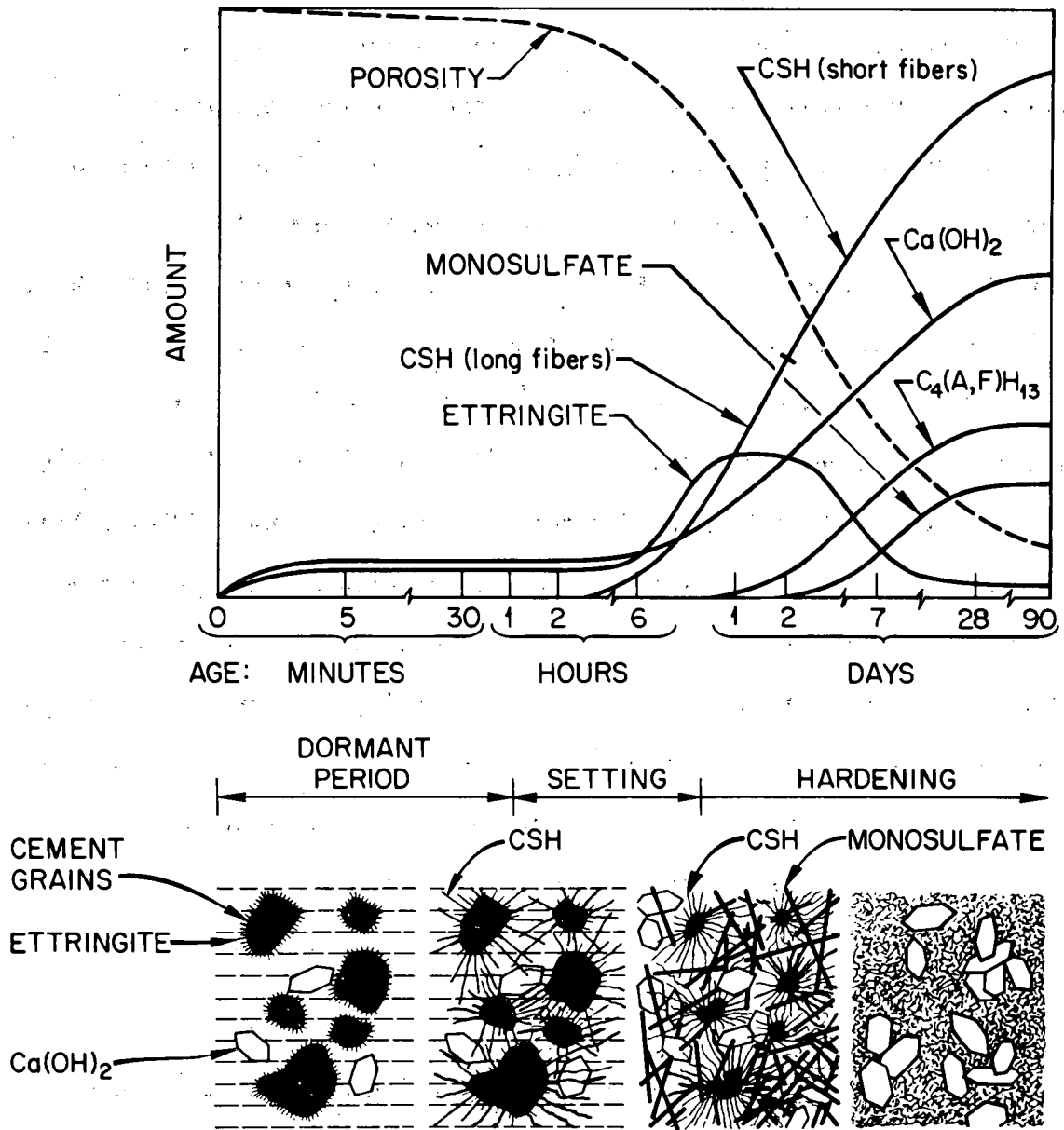
Table 10. Possible phases found in MCC-1 FUE-TAP concrete containing SRP-4 waste

Phase	Elements	
	Major	Minor
Zeolite	Cs, Si, Al	K, Ca, Ce, Fe
Gd ₂ O ₃	Ca, Fe, Gd	Cr, Fe, Si, Al, S
Fe ₂ O ₃	Fe	Ca, Si, Al, S
SiO ₂ (quartz - sand)	Si	-
Ni	Ni	-
Mn (contains Sr)	Mn	Sr
Cement phases:	Ca, Si, Al, Fe	S, K, Ti
	Si, Al, S, Fe	Ca, K, Na, Cs
	Ca, Si, Al, Fe	Mg, S, K, Ti
(calcium aluminate hydrate)	Ca, Al, Fe	S

material can be isolated (see Fig. 15);* thus, it is nearly impossible to identify the partitioning of radionuclides. For such identification, it may be necessary to examine microstructures as they hydrate.

Particles of C₃S*, C₂S, C₃A, and C₄AF could be identified in samples just beginning to hydrate. We would expect to see the radionuclides present in the very basic Ca(OH)₂ solution at this point. As hydration of the cementitious phases proceeds, the movement of radionuclides might be monitored.

*Cement-technology notation, where C = CaO, S = SiO₂, A = Al₂O₃, F = Fe₂O₃, and H = H₂O.



DRAWING FROM PORTLAND CEMENT PASTE AND CONCRETE
by I. Soroka

Fig. 15. Individual phases of hardened cement as a function of time.

5. LEACHABILITY

The leachability of the waste form during interim storage, transportation to the repository, and final placement in the repository in the event of an aqueous intrusion at any of the above points has been considered to be a principal parameter in SRP waste form selection. The leachability studies for SRP FUETAP specimens were conducted under both static and dynamic conditions, using the standard Materials Characterization Center MCC-1 static leach test²⁰ and the modified International Atomic Energy Agency (IAEA) leach test,²¹ respectively. Distilled water was selected as the base line for these studies. Standard MCC-1 silica water and brine leachants were assumed to represent solutions that might be encountered in real-life situations. The leachabilities of the individual radionuclides have a complex interrelationship between the cement type, setting properties, the waste composition, and the inclusion of specific fixatives such as clays. Various tests have been performed to determine the effects of these parameters on leachability. The results of these tests, which are presented in detail in a supplement,¹⁸ are summarized in this section.

Initially, conservative leach studies were made using the modified IAEA leach procedure, which exposes the specimens to fresh leachants throughout the test. Results indicated that leach rates (unnormalized) were on the order of $\leq 10^{-6}$, $\leq 10^{-4}$, and $\leq 10^{-8}$ g/(cm²·d) for cesium, strontium, and plutonium, respectively.

Typical values for the MCC-1 static leach tests are given in Table 11. Most of the leach rates for the MCC-1 static tests are reported as

Table 11. Typical values for the MCC-1 28-d leach rates from SRP FUETAP specimens in deionized water

Element	Leachant temperature (°C)	Leach rate ^a [g _i /(m ² ·d)]	
		Low	High
Al	90	1.6	5.7
Cs ^b	90	11.0	29.0
Fe	90	0.002	0.016
Mn	90	0.00096	0.027
Pu	25	0.011	0.40
Sr	90	0.113	0.830

^ag_i = reduced grams = grams of ith element divided by the mass fraction of that element in the waste.

^bCesium loaded on the zeolite Ionsiv IE-95.

average values and are based on the normalized or reduced mass (g_i) of the specimen. These reduced leach rates are calculated by:

$$LR_i = \frac{M_i}{f_i \cdot SA \cdot d} = \frac{W_0 \cdot A_i}{A_0 \cdot SA \cdot d},$$

where

LR_i = leach rate of element [g_i/(m²·d)],

M_i = mass of element in leachate (g),

f_i = mass fraction of element in initial specimen,

A_i = radioactivity of isotope i in leachate (counts/min),

A₀ = radioactivity of isotope i in initial specimen (counts/min),

W₀ = initial mass of specimen (g),

SA = surface area of specimen (m²), and

d = leaching time (d).

Since the pH of typical cement-based waste host leachants is high (11.5 to 12.5), the solubilities (and therefore the leachabilities) of actinides in static tests are very low [$<10^{-2}$ $g_i/(m^2 \cdot d)$]. The leachabilities of the short-lived fission products (cesium and strontium) are controlled by tailoring the formulation of the mix to the specific waste stream. The effects of substituting clay for sand (MCC-3 and MCC-4 mixes) are shown in Table 12. Clay additives reduce the initial cesium washout by a factor of 2. A statistical analysis of 70 uranium MCC-1 leach tests (Appendix B) showed a significant difference in uranium concentrations in leachates between waste formulations containing 3.5% Indian red pottery clay (MCC-6A mix) and those containing bentonite clay (MCC-6B mix). The Indian red clay had a significantly lower uranium leach rate. Additional tests were made to determine the effects of cement type (Table 13 and Fig. 16). The data from these tests confirm that the FUETAP process yields acceptable product with any of the three, readily available commercial cements. The dependence of leachability on leachant and leaching temperature is shown in Table 14. Only the leaching of strontium into silica water shows a statistically significant difference for the temperatures of 40 and 90°C. The reference waste composition for Tables 12 and 13 is SRP-4, while that for Table 14 is SRP-6 (Table A.2, Appendix A). The latter waste required a larger amount of water to produce a processible mix and yielded a final product with 50% greater porosity than the former waste. As a result, the cesium washouts from the SRP-6 waste form were higher (four to five times); therefore, the 28-d leach rates for cesium are higher in Table 14 than in Table 12.

Table 12. Effects of Indian red pottery and bentonite clay additives on the leach rate of cesium from FUETAP concretes

Leach time (d)	Cesium MCC-1 leach rates ^a at 90°C [$g_i/(m^2 \cdot d)$]					
	DIW leachant ^b			SIW leachant ^c		
	MCC-3 mix ^d	MCC-4 mix ^e	MCC-1 mix ^f	MCC-3 mix ^d	MCC-4 mix ^e	MCC-1 mix ^f
3	85	97	150	89	63	99
7	44	53	81	50	30	52
14	27	35	44	25	19	35
28	-	-	29	-	-	16

^a g_i = reduced grams = grams of ith element divided by the mass fraction of the ith element in the waste.

^bDIW = distilled water.

^cSIW = silica water.

^d7.0 wt % Indian red clay substituted for sand.

^e3.5 wt % Indian red clay plus bentonite clay substituted for sand.

^fNo clay added to mix.

Table 13. Effect of cement type on MCC-1 28-d leach rates from FUETAP specimens in deionized water

Cement type	28-d MCC-1 leach rates ^a at 90°C [$g_i/(m^2 \cdot d)$]			
	Al	Fe	Mn	Sr
Type I Portland	3.31	0.0041	0.00096	0.43
Type IS slag	1.57	0.0020	0.0234	0.39
Fondu (high alumina)	5.67	0.0091	0.0152	0.83
50% Type I + 50% Fondu	4.11	0.0159	0.0268	0.11

^a g_i = reduced grams = grams of ith element divided by the mass fraction of the ith element in the waste.

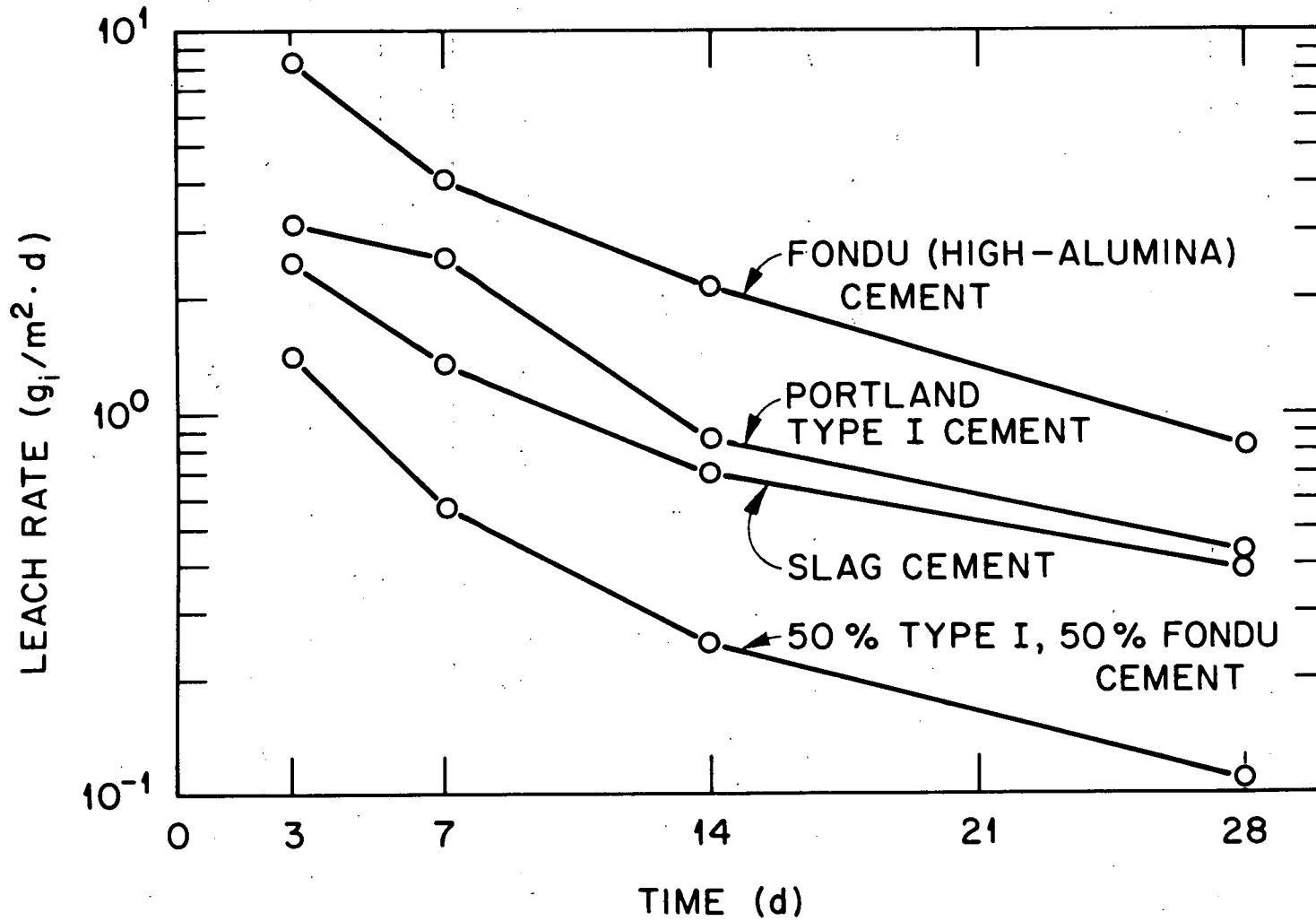


Fig. 16. Strontium leach rates for three cements in four MCC-1 formulations using MCC-1 static leach test at 90°C with distilled water.

Table 14. Effect of temperature^a on leach rates^b from MCC-6A FUETAP specimens^c

Leachant	Temperature (°C)	$g_i/(m^2 \cdot d)$				
		Cs	Sr	U	Ce	Nd
Distilled water (DIW)	90	48 ± 7	0.27 ± 0.02	0.035 ± 0.008	0.11 ± 0.02	<0.1
Silica water (SIW)	40	46 ± 3	1.3 ± 0.1	0.007 ± 0.003	0.02 ± 0.02	<0.1
	90	37 ± 3	0.30 ± 0.01	0.02 ± 0.01	0.02 ± 0.01	<0.1
Salt brine (BRI)	40	59 ± 12	17 ± 6	0.06 ± 0.01	<0.1	1.0 ± 0.5
	90	53 ± 5	23 ± 5	0.06 ± 0.01	<0.1	0.6 ± 0.2

^a28-d MCC-1 leach test at 40 and at 90°C.

^bLeach rates in $g_i/(m^2 \cdot d)$, where g_i = reduced grams = g of *i*th element divided by the mass fraction of the *i*th element in the waste.

^cPlus and minus values are one standard deviation.

Results of recent tests have shown that increasing the calcining and curing temperatures can reduce the initial cesium washout. The SRP waste solids would normally be calcined at 600°C before being mixed with concrete additives in the first step of Fig. 1. Mild curing temperatures and pressures (100°C, 0.1 MPa) were used for most tests since the physical properties of FUEAP concretes are not improved by increasing the curing time, temperature, or pressure (Sect. 2.3). The data in Table 15 show that increasing the waste solids calcining temperature to 900°C and the concrete curing temperature to 200°C would significantly lower the initial cesium washout and would thus reduce the leach rates.

Table 15. Initial cesium release from SRP FUEAP specimens^a after 3-d leach with deionized water at 90°C

Curing temperature (°C)	Cesium release ($\mu\text{g}/\text{cm}^2$) at calcining temperature of	
	600°C	900°C
85	21	9
	20	17
100	19	13
	18	12
200	6	4
	7	-

^aCesium loaded on the zeolite Ionsiv IE-95.

The MCC-1 standard leach test²⁰ is a static system. As such, the leachate concentrations approach and eventually achieve saturation. The MCC-1 procedure requires that all "leach rates" be reported at an arbitrary leach time of 28 d. Therefore, the MCC-1 28-d "leach-rate" values may only represent saturated leachate concentrations divided by 28 d. This is clearly indicated in Table 14, where the concentrations of uranium, cerium, and neodymium in the leachates were constant throughout the 3-, 7-, 14-, and 28-day tests. The statistical analysis of the results from 70 uranium MCC-1 leach tests (Appendix B) also shows that the uranium concentrations have no significant time-dependence in these tests. Furthermore, there was no statistically significant difference in uranium solubility between deionized water and silica water leachants; however, brine holds more uranium in solution. Uranium solubility was statistically the same at 40 and 90°C in the brine, but showed a significant increase with temperature in the silica water.

The MCC-1 procedures provide for measurement of "leach rates" by a plot of normalized elemental mass losses vs time. The normalized elemental mass loss is:

$$(NL)_i = \frac{M_i}{f_i \cdot SA} ,$$

where

$(NL)_i$ = normalized elemental mass loss (g/m²),

M_i = mass of element i in the leachate (g),

f_i = mass fraction of element i in the unleached specimen,

SA = geometric surface area of the specimen calculated by using overall dimensions (m²).

If there is no initial wash-off, these plots will go through the origin. The MCC-1 sample preparation procedures allow cutting, polishing, and ultrasonic washing in order to eliminate wash-off from the surfaces of glass and other nonporous waste hosts. In the case of concretes, these procedures may actually increase the initial wash-off.

Figures 17 and 18 illustrate the effects of initial wash-off on reported MCC-1 leach rates for strontium and cesium, respectively, from MCC-1 FUETAP concrete at 90°C. Cesium has a much higher initial wash-off, which can be substantially reduced by increasing the calcination and curing temperatures or by the addition of clays as described above. When these short-term leach rate data are reported as specified in the MCC-1 testing procedure, the results are biased by the initial wash-off.²²

In the MCC-1 procedure the size and shape of the solid test specimen are not considered critical and are left to the user's choice. Therefore, an unspecified assumption that the test specimen is to be treated as a semi-infinite solid is implied. In the case of diffusion-controlled leaching, laboratory results can be scaled to larger monoliths by using the test specimen's surface/volume ratio (SA/V). The data presented here involved test specimens with SA/V ratios of ~7, while engineering-scale waste forms have a SA/V of <0.1. Therefore, 55-gal monoliths would have fractional release rates that are smaller, by a factor >70, than those presented here. Our results indicate that the MCC-1 static leach procedures give no insight into the long-term leaching behavior of large-scale concrete blocks.^{21,23}

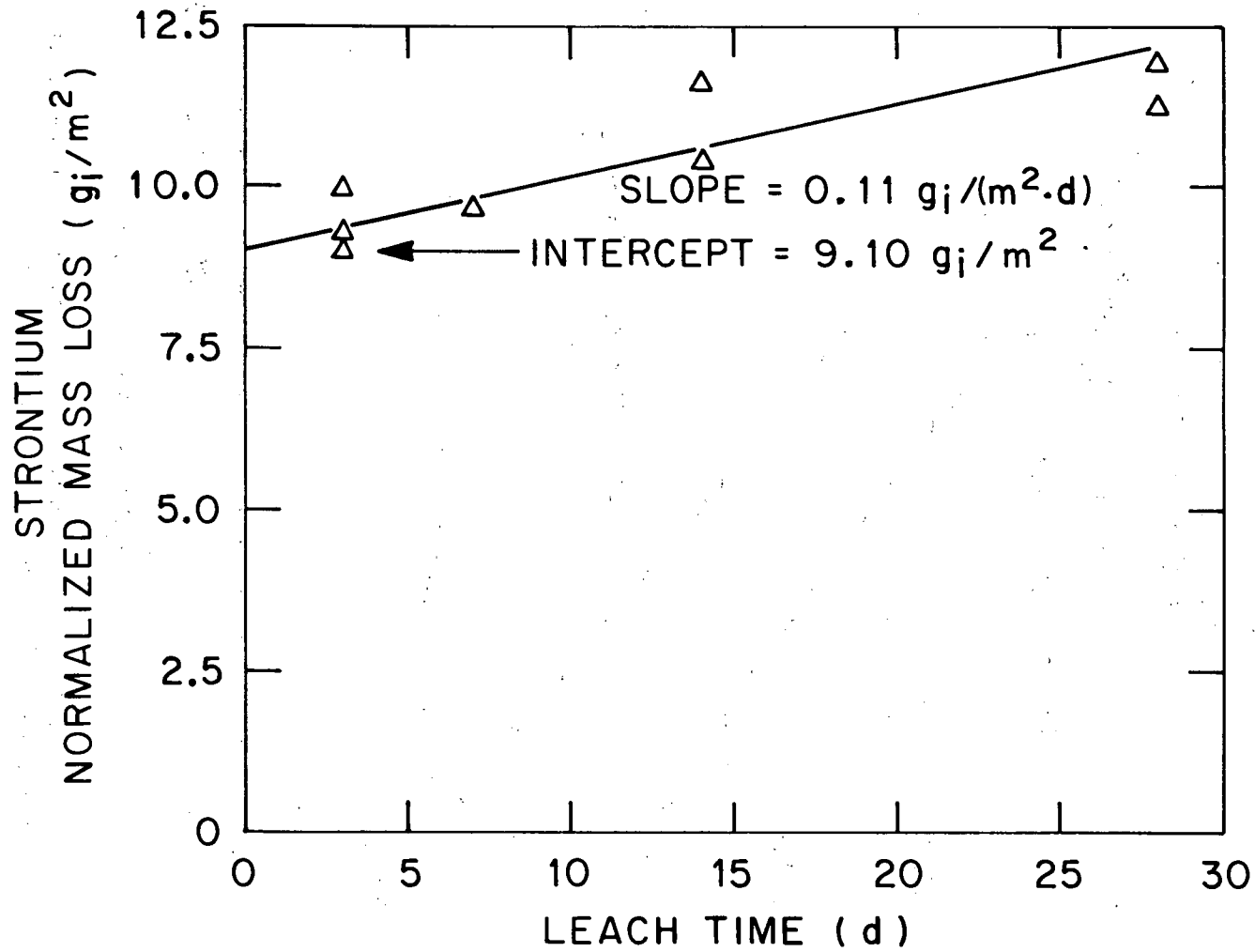


Fig. 17. MCC-1 strontium leach results at 90°C in deionized water for MCC-1 FUETAP concrete containing SRP-4 simulated waste.

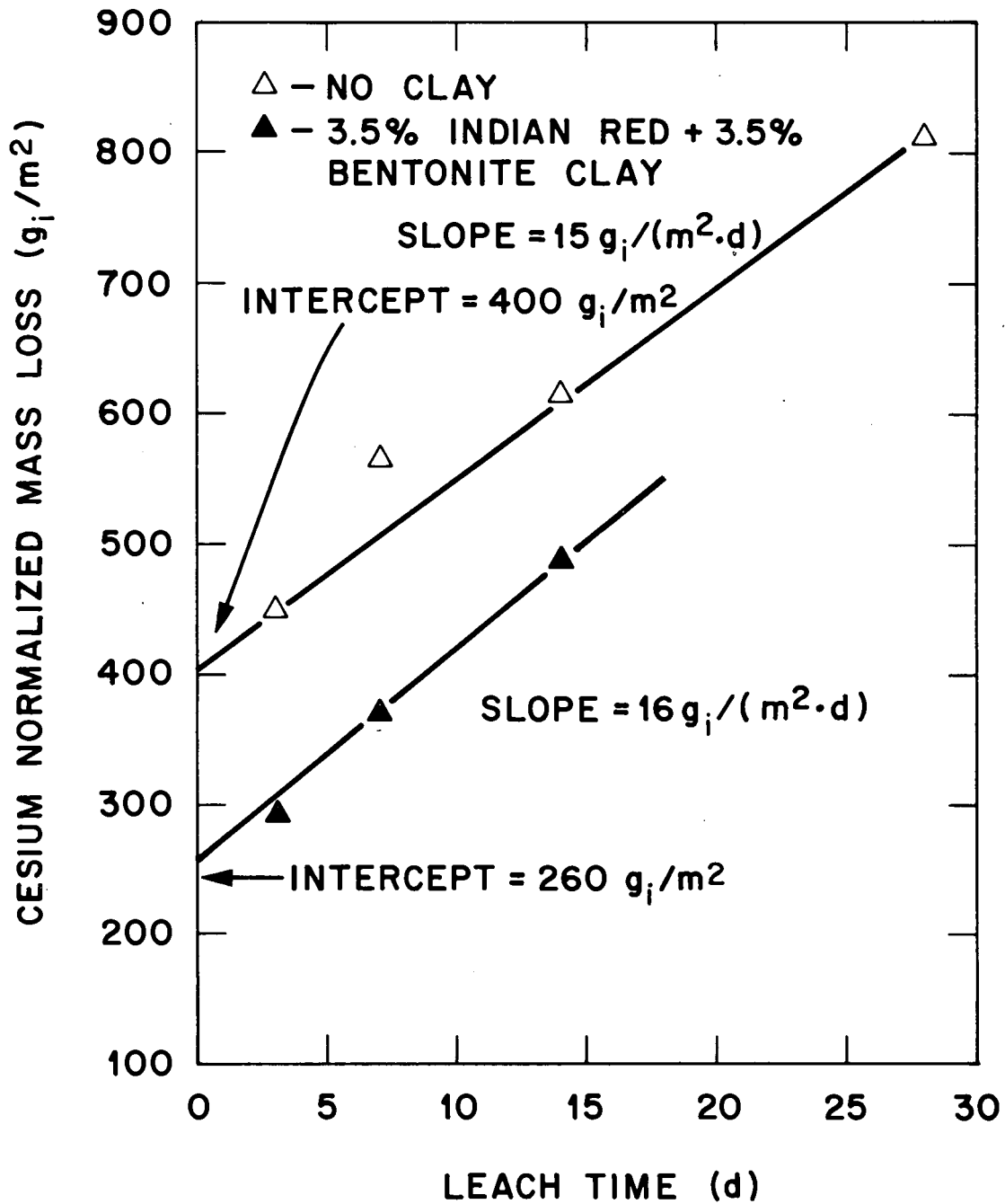


Fig. 18. Effects of clay additives on cesium leach rates from FUETAP concrete (MCC-1) in deionized water at 90°C.

6. THERMAL STABILITY

Thermal studies were made to determine the effects of increased temperature on FUETAP concrete specimens during transportation and during storage in an approved facility. The effects of fire were examined assuming that the maximum temperature experienced by the waste solid would be 800°C. Results of the thermal stability studies demonstrated that prolonged heating (>2 years) of simple concretes at the expected operating temperature of a waste storage facility (100°C) produced only minor changes in compressive strengths. Also, concrete-sludge samples showed no loss of mechanical integrity after prolonged heating at 400°C.²⁴ Results of ORNL studies performed at 250°C show that FUETAP specimens have an ~1.4 wt % loss and a 10% reduction in compressive strength during the first month but no significant change after that.

In short-term heating tests, the FUETAP concrete specimens were found to be thermally stable up to 900°C, the maximum temperature used in the laboratory studies. After 24 h at 900°C, they contained only ~1 wt % water and had a volume reduction of ~1.7%. Although a few hair-line fractures were evident, the specimens had adequate compressive strengths (~20 MPa).

Thermal expansion measurements were made to determine the thermal expansion coefficient using a series of samples, each of which was approximately 15 mm in diameter by 31 mm long. These samples, which were prepared by using the MCC-1 formulation with SRP-4 waste solids, were cured and dewatered by the standard FUETAP method (100°C - cure; 250°C - dewater; 24 h each).

A Harrop thermal dilatometric analyzer (Model TD-712) connected to a Harrop differential thermal analyzer (Model TA-700) was used to perform and record the thermal expansion experiments. The system was calibrated at the heating rate of 4°C per minute using a 2.00-in. alumina standard. The recorder is calibrated to plot thermal expansion as a percent of the initial length vs sample temperature.

The sample was subsequently placed in the thermal dilatometric analyzer, where it was heated at the rate of 4°C per minute to 800°C, held at 800°C for ~5 min, and then returned to room temperature at the rate of 4°C per minute.

Figure 19 shows a typical expansion curve for a FUETAP sample prepared from MCC-1 mix and SRP-4 waste. During the heating cycle, the length of the sample increased almost linearly up to ~0.2% at 400°C and then continued to increase gradually up to ~580°C. This expansion was caused by the transition from alpha to beta quartz in the sand aggregate. The sample length remained fairly constant between 600 and 700°C, after which it began to shrink rapidly. At 800°C, the sample expansion was ~-0.7%. Upon cooling, the sample shrank linearly until a sharp drop occurred at ~580°C, caused by the reversible transition from beta to alpha quartz. At room temperature, the final sample length was 1.7% less than the original length.

Using the expansion curve in Fig. 19, the average value of the linear thermal expansion coefficient was found to be $4.7 \times 10^{-6}/^{\circ}\text{C}$ between 20 and 400°C, which is approximately half that of most HLW glasses and hard-rolled steel. The transition between alpha and beta

ORNL DWG 81-547R

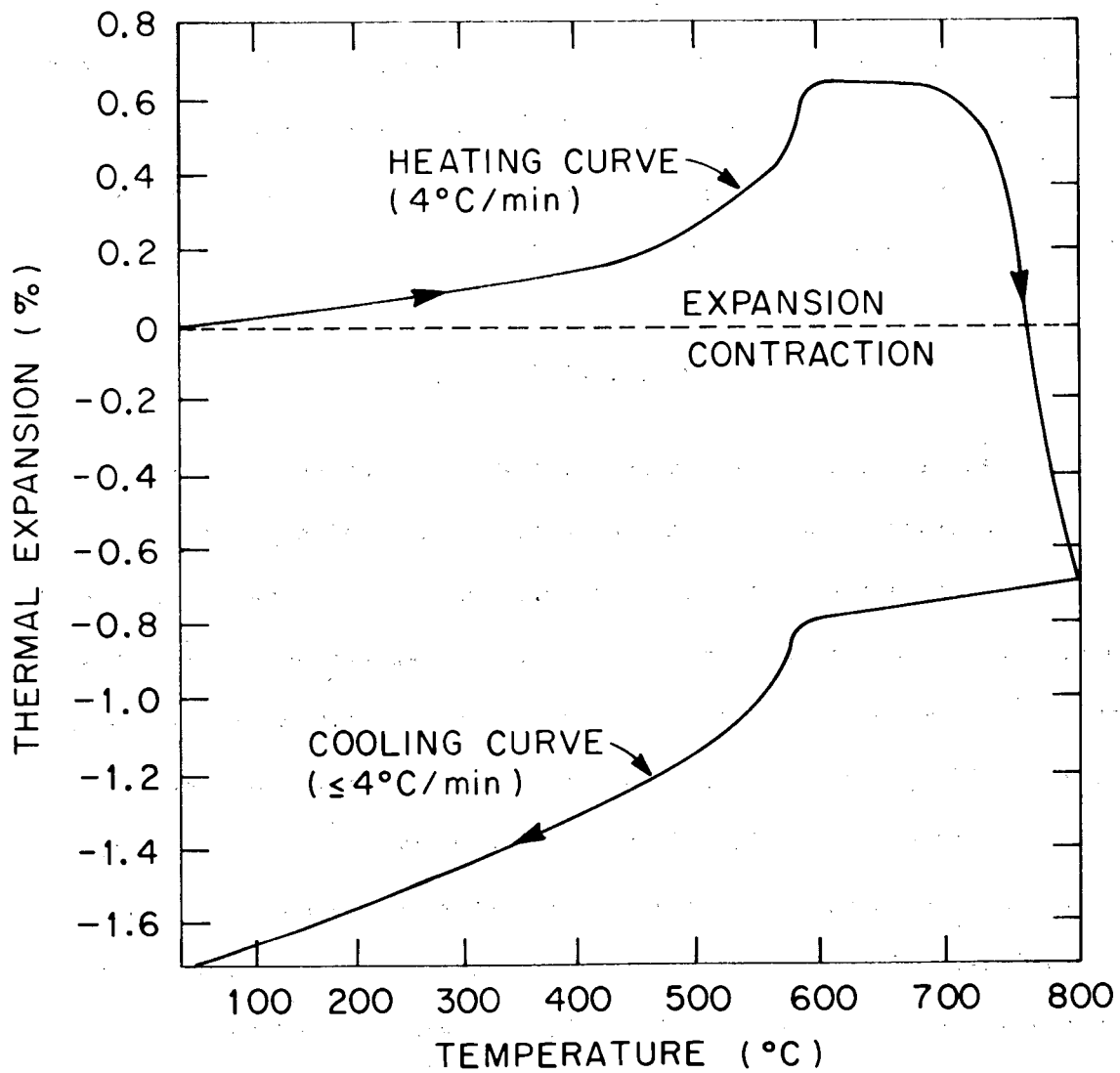


Fig. 19. Typical expansion curve of MCC-1 SRP FUETAP concrete specimens.

quartz at 580°C resulted in a maximum expansion in length of 0.65%. The FUETAP concrete expanded a maximum of 2.0 vol % at 580°C and then began to shrink at 700°C. At 800°C, the volume was approximately 2.2% less than the initial value. The net volume change after cooling was -5%, and the final weight loss was ~-8%. The compressive strength remained at 20 MPa. The gases produced during the heating cycle are water and carbon dioxide, primarily from the decomposition of Ca(OH)_2 and CaCO_3 , which are by-products of cement hydration.

7. RADIATION STABILITY

The radiolysis of cement-pore water and the potential pressurization of waste canisters due to an accumulation of the radiolytically produced gases have been identified as major concerns for radioactive waste hosts. By linear extrapolation of short-term experiments (<5 months), Bibler²⁵ estimated that a gas buildup to ~100 atm (10 MPa) could occur after 100,000 years in a standard canister containing alpha waste. Long-term radiolysis studies (>500 d) made at ORNL show that the gas generation rate does not remain linear with time. Each of the gas generation-vs-time plots has a steep, initially linear portion (seen by Bibler) and then levels off. These longer-term studies demonstrate that Bibler's model grossly overestimates the long-term pressure and that radiolysis of concretes is not a serious problem and does not limit their application to radwaste management.

The radiolysis of concrete is dependent on the amount of unbound or free water present in the system. Therefore, removal of all or most of

this water will greatly reduce or eliminate the gaseous radiolysis products. Unbound water is removed from the FUETAP concretes during the autoclave curing step (Sect. 2). Results of laboratory studies have demonstrated that the dewatered concretes contain only 2 wt % water, which is chemically bound in the cement's hydration products. Regardless of the production rate, however, pressurization from the accumulation of hydrogen and oxygen is avoided when sufficient recombination of these gases occurs during their generation. Tests have been made on undewatered and dewatered FUETAP samples to determine both the long-term (2- to 4-year) alpha-radiolysis gas generation and the effectiveness of FUETAP concrete as a recombination catalyst for hydrogen and oxygen. The results, which are detailed in a supplement,¹⁹ are summarized in this section.

In the long-term (>500-d) radiolysis experiments performed at 25 to 30°C, we used 10-cm³ steel capsules containing FUETAP concrete specimens (1.5 cm diam x 3.5 cm long; 6.2 cm³; 8.2 g of solids) which were spiked with 4.5 mg (tests 1 through 3), 0.5 mg (tests 4 and 5), and 1.5 mg (test 6) of curium-244 (12.3 mg/Ci). Each test day was equivalent to 300, 30, and 100 years, respectively, in the life of a real waste drum (based on an estimated alpha dose of 6 rad/h for SRP waste). The dead volume (~5.8 cm³) of each test cell was measured by expanding a known volume and pressure of argon into these test capsules.

The results of these experiments show that the pressure increases do not remain linear with time and that the equilibrium pressures are dependent on both dose rate and temperature. Tests performed for

periods as long as 400 d at 5.6×10^5 rad/h showed that the drum pressure would level off at 30 psig after a dose of 55,000 dose-equivalent years. Table 16 summarizes the radiolysis gas generation data. The total gas (molecules/100 eV) values were taken from the averages of the initial linear slopes of the pressure rises and are very conservative overestimates of the long-term gas generation. These total gas values are one-fifth to one-third of Bibler's estimated values.²⁶

Table 16. Results of FUETAP alpha-radiolysis tests with ^{244}Cm

Test	Conditions for dewatering (250°C, 24 h)	Dose rate (rad/h)	Total gas ^a (molecules/100 eV)	Average range (dose-equivalent years) ^b
1	No	5.6×10^5	0.095 ± 0.005^c	300-15,000
2	Yes	5.6×10^5	0.006 ± 0.002	2,000-50,000
3	Yes	5.6×10^5	0.005 ± 0.002	300-50,000
4	Yes	6.3×10^4	0.001 ± 0.0008	7,000-16,000
5	Yes	6.3×10^4	0.002 ± 0.001	1,500-7,500
6	Yes	1.9×10^5	0.008 ± 0.005	2,700-10,000

^aTaken from the initial linear portion of the plot showing pressure rise with time.

^bBased on an estimated alpha dose of 6 rad/h for SRP FUETAP formulas.

^cStandard deviation.

Figure 20 presents the estimates of gas pressurization for undewatered and dewatered FUETAP (tests 1 through 3) concretes in a 200-L drum filled to 90% capacity. These data show that the first 1000 equivalent years of accelerated dose to undewatered FUETAP concrete

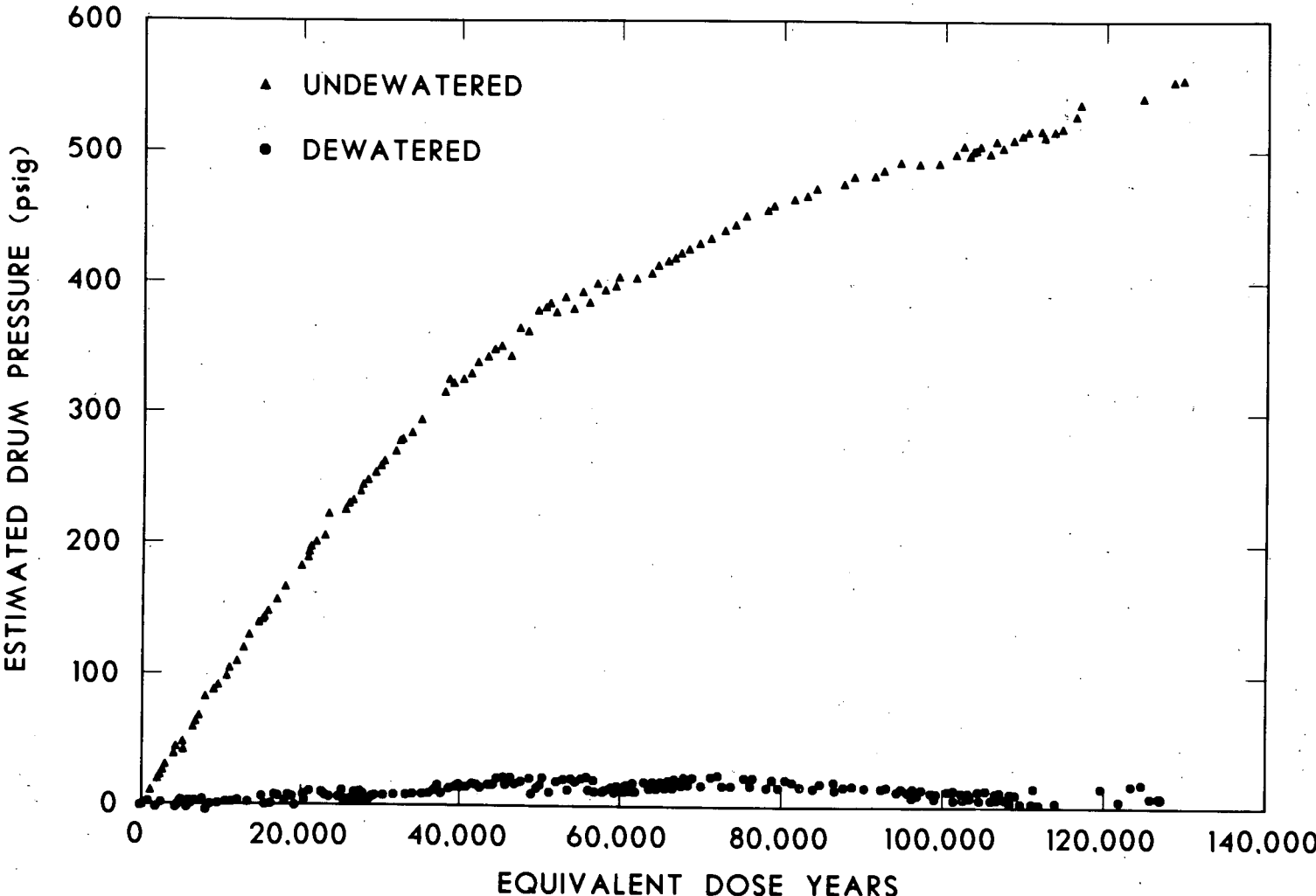


Fig. 20. Comparison of gas generation rates of SRP FUETAP concrete before and after dewatering (tests 1 through 3).

results in a drum pressure of 14.6 psig in the undewatered case and negligible pressures in the dewatered cases. Furthermore, this small radiolytic gas production is dose dependent and is expected to be lower for real waste. Test specimens were spiked with ^{244}Cm from a nitric acid solution, resulting in a homogeneous curium distribution. However, real waste has most of its alpha activity bound in large agglomerates which reduce the actual alpha dose to the cement by a factor of 100 via self-absorption. Also, the use of small specimens results in a loss of the recombination effects because their diffusion paths are unrealistically short. Depending on the test geometry and the spiking procedure, data from tests such as these may overestimate the actual radiolysis by factors between 3 and 1000.

Figure 21 summarizes the pressure-vs-time data for an undewatered FUETAP (test 1). These results disprove the efficacy of the linear extrapolation of the alpha-radiolysis gas generation data taken from short-term (<200-d) tests. Also, they show that the recovery of the pressure after gas sampling at day 500 is approximately superimposable on the initial rise from 90 to 130 psig. No significant change in the radiolysis character after 150,000 equivalent years of exposure is noticeable. The rate of the recombination reaction appears to balance the radiolysis rate, producing a maximum pressure limit. Such information indicates that measurements of radiolysis rates are dependent on the arbitrary choice of the geometry and the dead volume of the test cell. Therefore, comparisons of radiolysis measurements between laboratories are not meaningful unless a standard geometry is used.

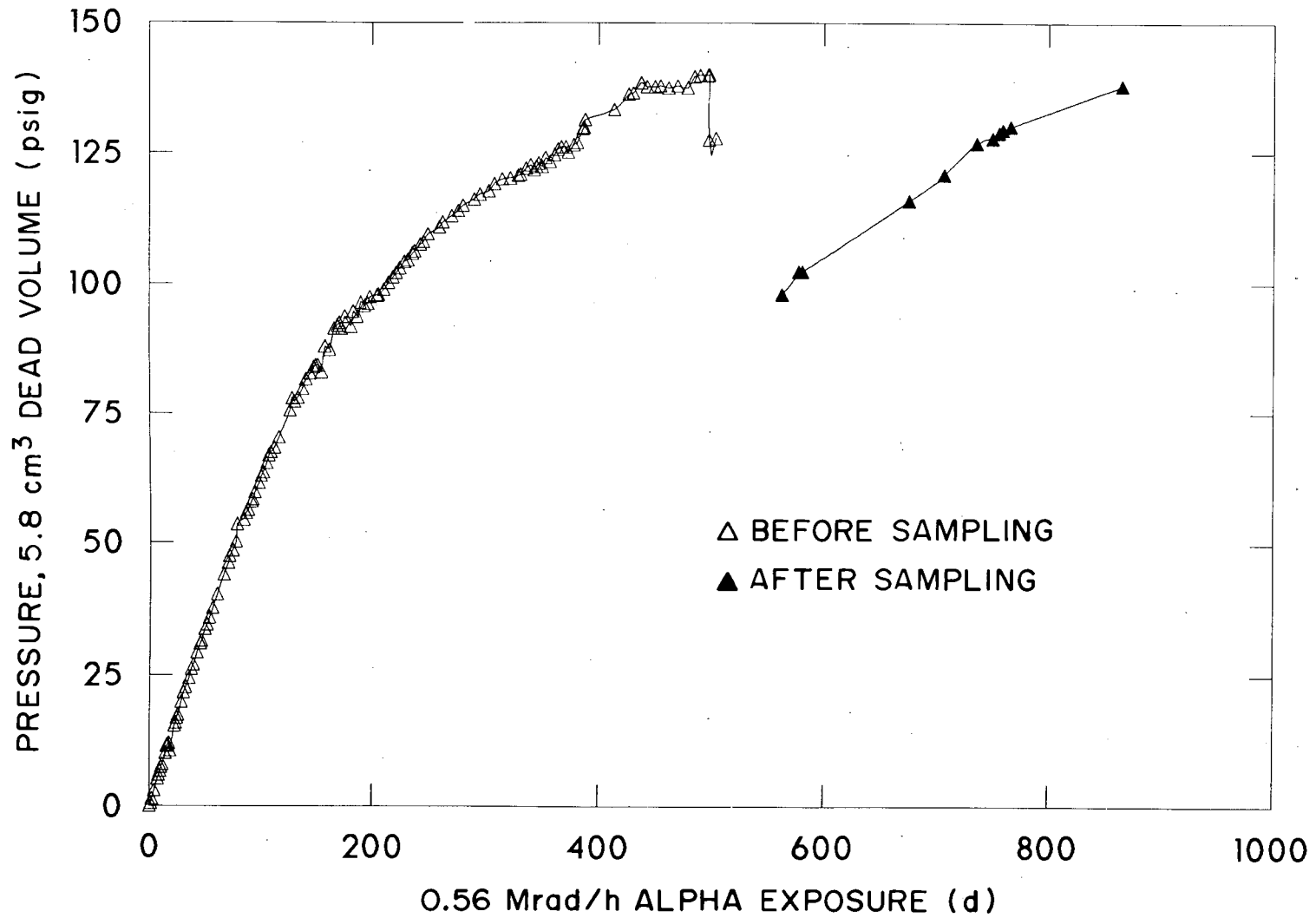


Fig. 21. Alpha radiolysis of undewatered SRP FUEAP concrete containing 4.5 mg of ^{244}Cm in 8.2 g of host solid with gas sampling after 500 d (test 1).

Figure 22 shows the results of duplicate tests of the alpha radiolysis of a dewatered FUETAP concrete with the same dose rate (0.56 Mrad/h) as test 1 (Fig. 21). The pressures generated in the dewatered samples are an order of magnitude lower than those for the undewatered sample. Pressure does fluctuate in the first 200 d, demonstrating a cyclical buildup and decrease of pressure and a corresponding catalytic recombination of hydrogen and oxygen. Gas sampling in test 2 at day 500 is shown in Figs. 23 and 24. The latter figure shows the pressure recovery superimposed on the initial buildup of radiolysis gas. Again, these results do not indicate a significant change in radiolysis character after 150,000 equivalent-years of alpha dose.

Figure 25 displays the results of tests 4 and 5 (duplicates) of the alpha radiolysis of a dewatered FUETAP concrete with a dose rate about one-tenth of that in tests 2 and 3. The expected pressure oscillations are seen in the data from test 4; however, the data from test 5 show no initial pressure oscillations and no significant pressure rise until ~250 d. Evidently, in test 5 the test chamber was not properly balanced at atmospheric pressure after the dead-volume calibration. Since the pressure transducer could not read negative pressures, such data indicate a negative base-line offset.

Figure 26 shows the alpha-radiolysis data of test 6 using a dewatered FUETAP concrete with a dose rate (0.19 Mrad/h) which was intermediate between the two dose rates of previous tests. The initial slope of the curve indicates a total gas (molecules/100 eV) value that is comparable to the values listed in Table 16. The pressure becomes significantly

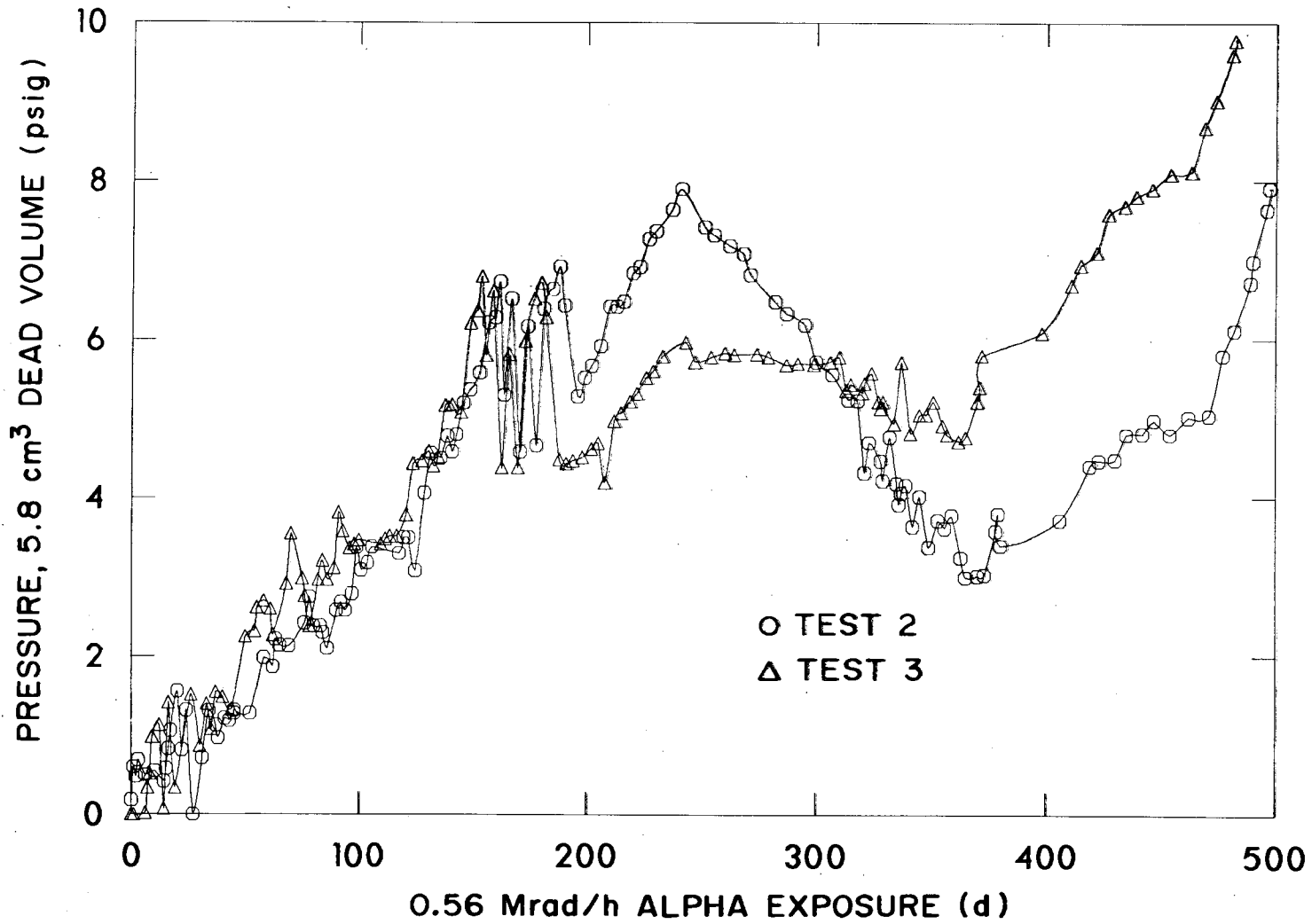


Fig. 22. Alpha radiolysis of duplicate dewatered SRP FUETAP concretes, each with 4.5 mg of ^{244}Cm in 8.2 g of host solid.

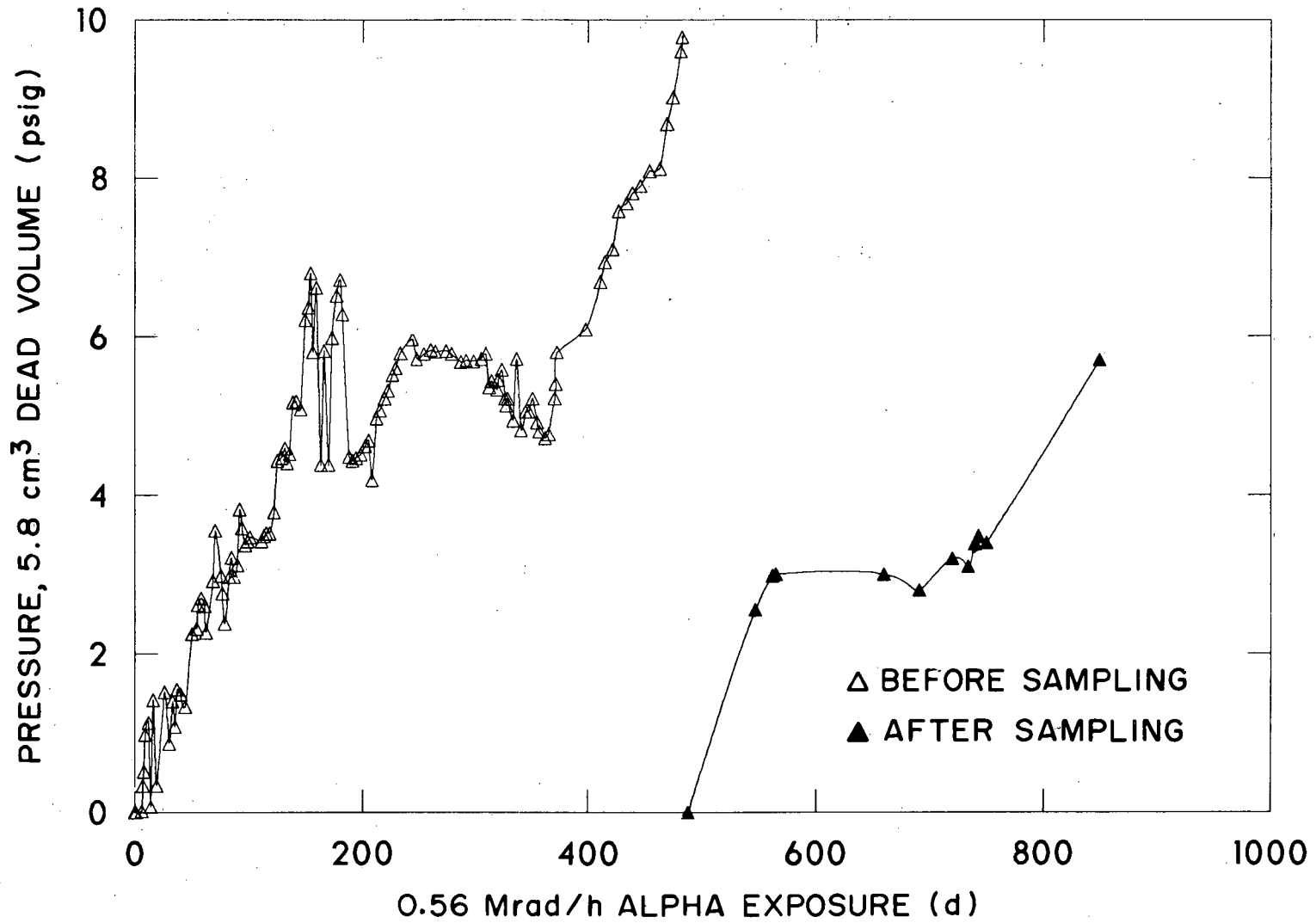


Fig. 23. Alpha radiolysis of a dewatered SRP FUETAP concrete with gas sampling after 500 d (test 2).

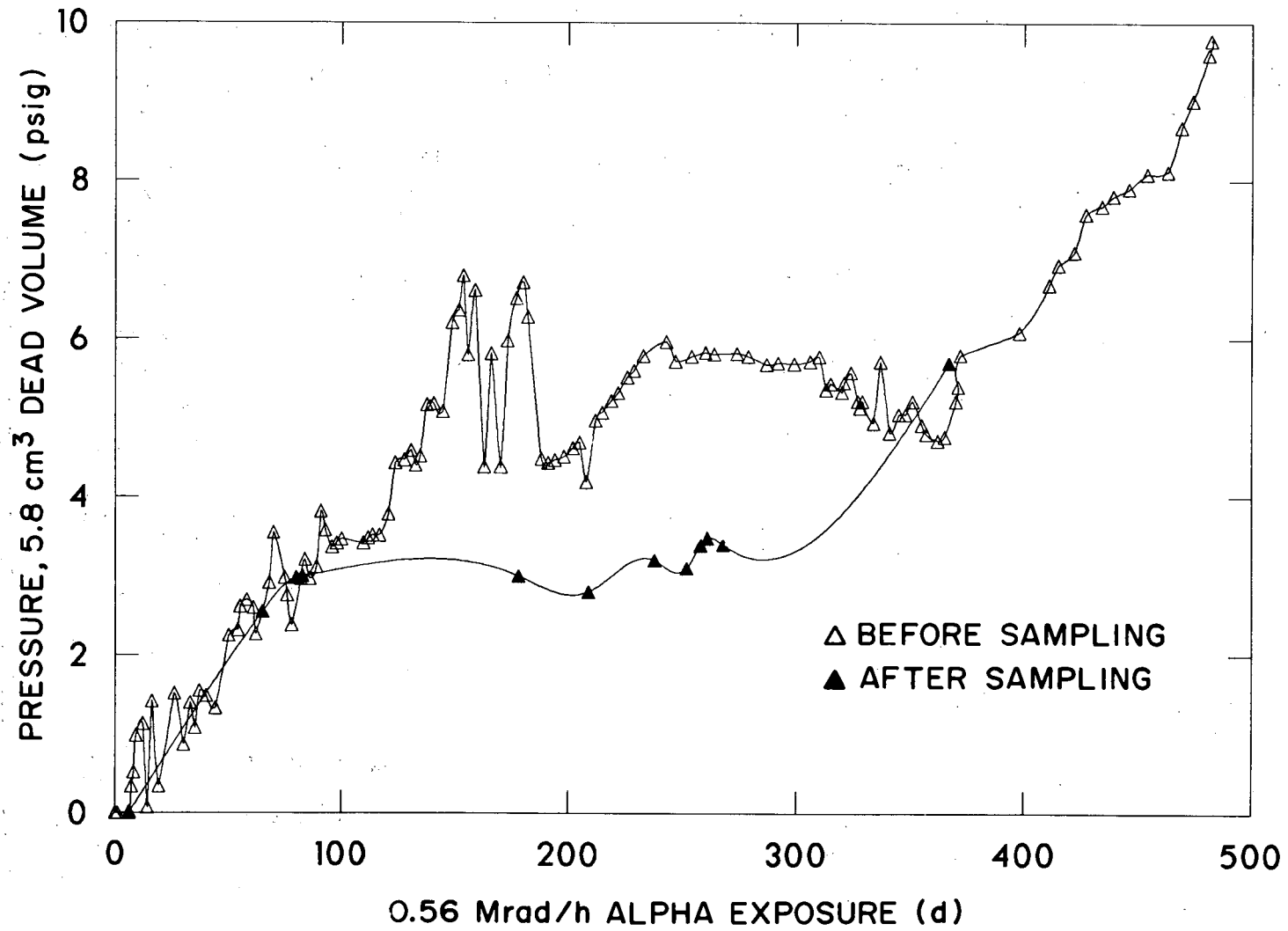


Fig. 24. Superposition of the pressure rise after gas sampling (test 2).

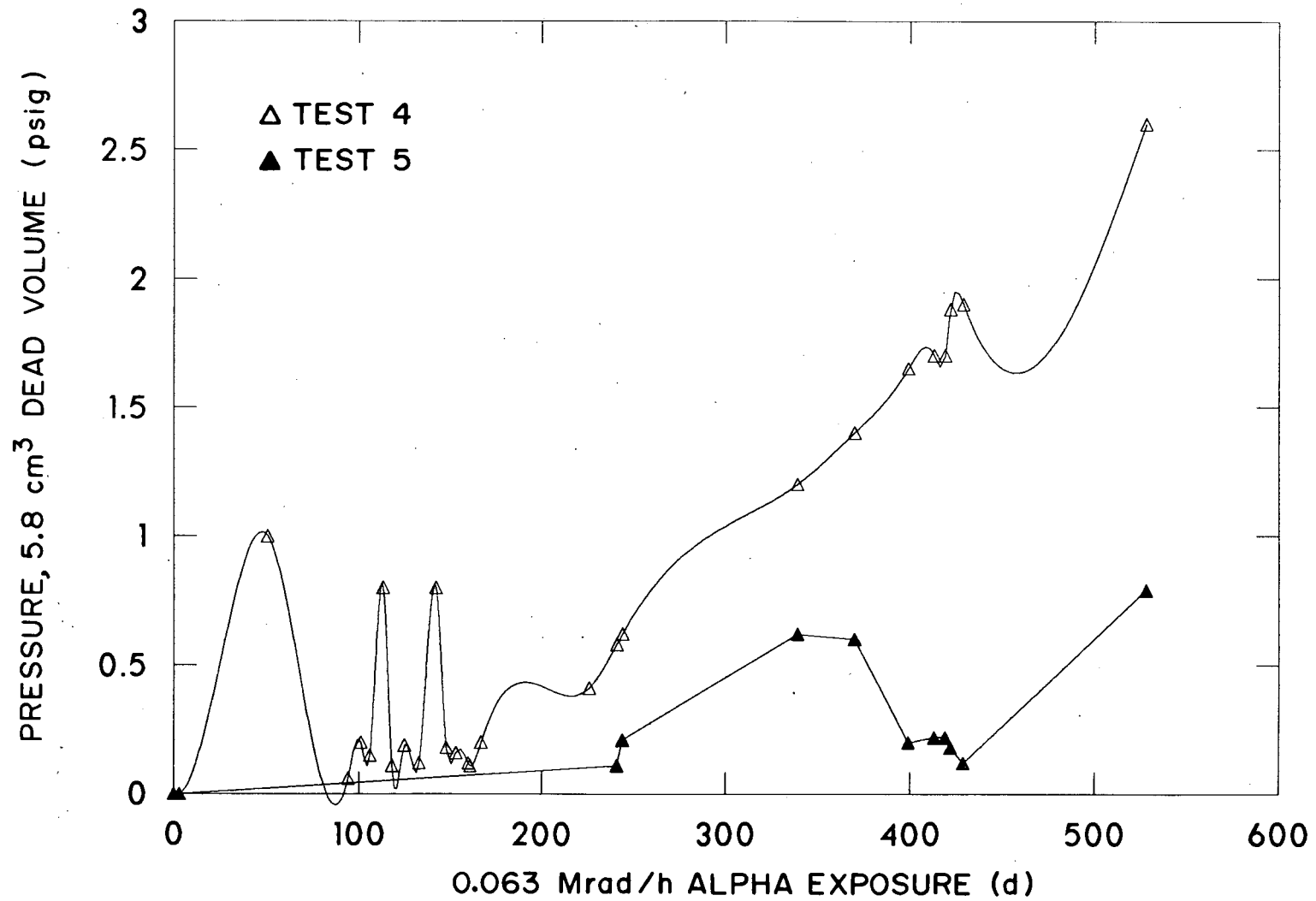


Fig. 25. Alpha radiolysis of duplicate dewatered SRP FUETAP concretes, each with 0.5 mg of ^{244}Cm in 8.2 g of host solid.

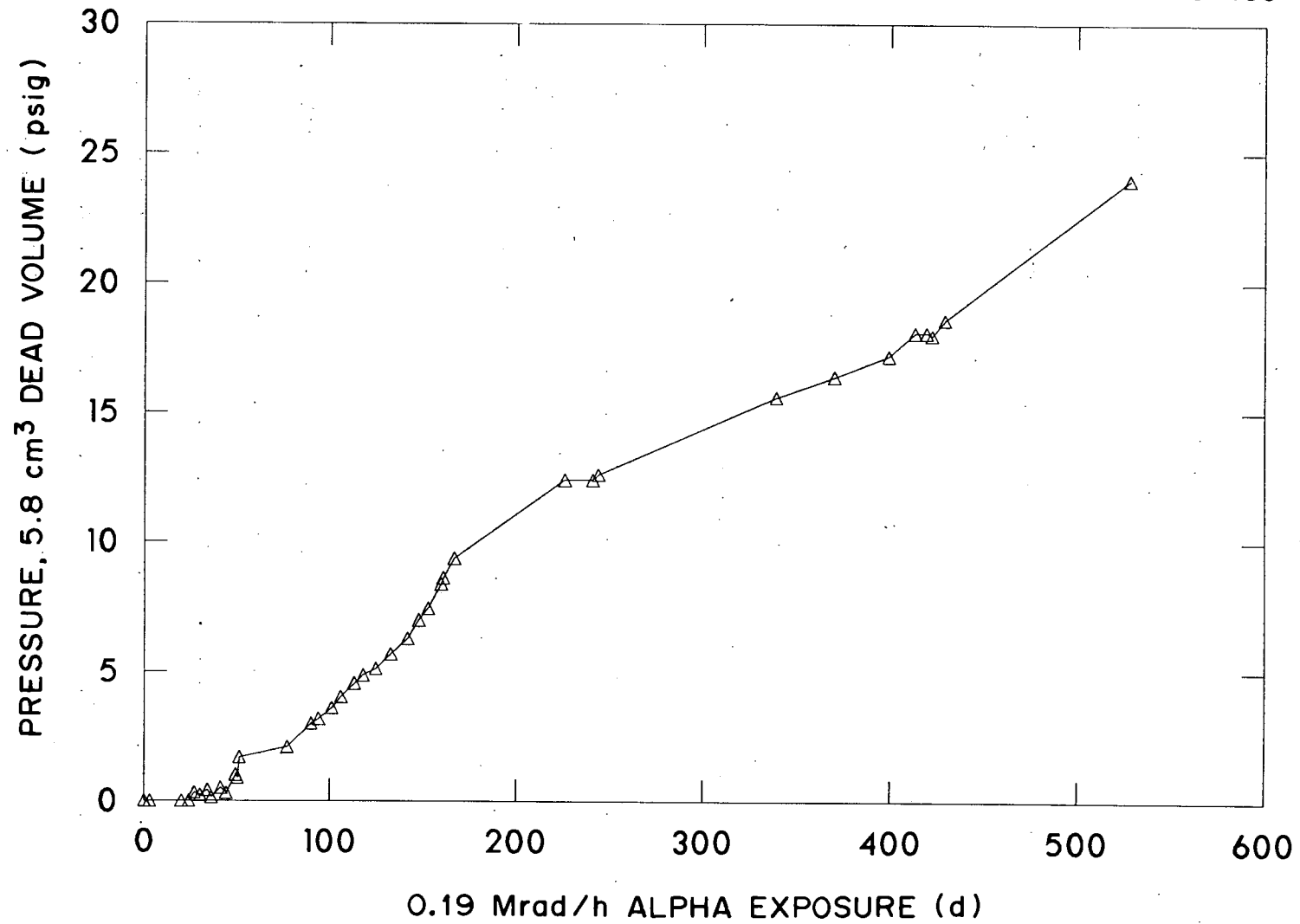


Fig. 26. Alpha radiolysis of a dewatered SRP FUETAP concrete containing 1.5 mg of ²⁴⁴Cm in 8.2 g of host solid (test 6).

higher than that observed in the other dewatered tests (tests 2 through 5) after 8000 to 9000 equivalent dose-years. Since the data exhibit no initial pressure oscillations and no positive pressure for the first 20 to 30 d, the test chamber was probably not properly balanced after the dead-volume calibration. The higher nonoscillating pressure suggests that the pressurization is from nitrogen alone, which implies that the surrogate waste used for this batch may have contained an unusually high nitrate concentration. No final analysis of the waste was made to confirm this possibility.

Figure 27 presents the data from tests 1 through 3 in volume (liters, STP) of gas generated per kg of host solid vs the equivalent dose-years in the life of a real waste drum (based on an estimated alpha-dose rate of 6 rad/h for SRP waste). This same information is shown in Fig. 20 as estimated drum pressure. The results for the dewatered samples (tests 2 through 6) at three different dose rates are shown in Fig. 28. These data, except for those of tests 5 and 6 (as noted previously) are effectively normalized by using an equivalent dose-years scale.

In the undewatered case after 500 d of alpha radiation (test 1), the volume % gas composition (Table 17) was typical for the radiolysis of water, with hydrogen and oxygen being the major species. However, nitrogen was the predominant species (96 to 98 vol %) in tests 2 and 3 with the dewatered FUETAP concretes (Table 17). These results substantiate the conclusions of Katz,²⁷ who showed that FUETAP concretes were very active hydrogen-oxygen recombination catalysts and suggested that these radiolysis products could not accumulate in the dewatered FUETAP

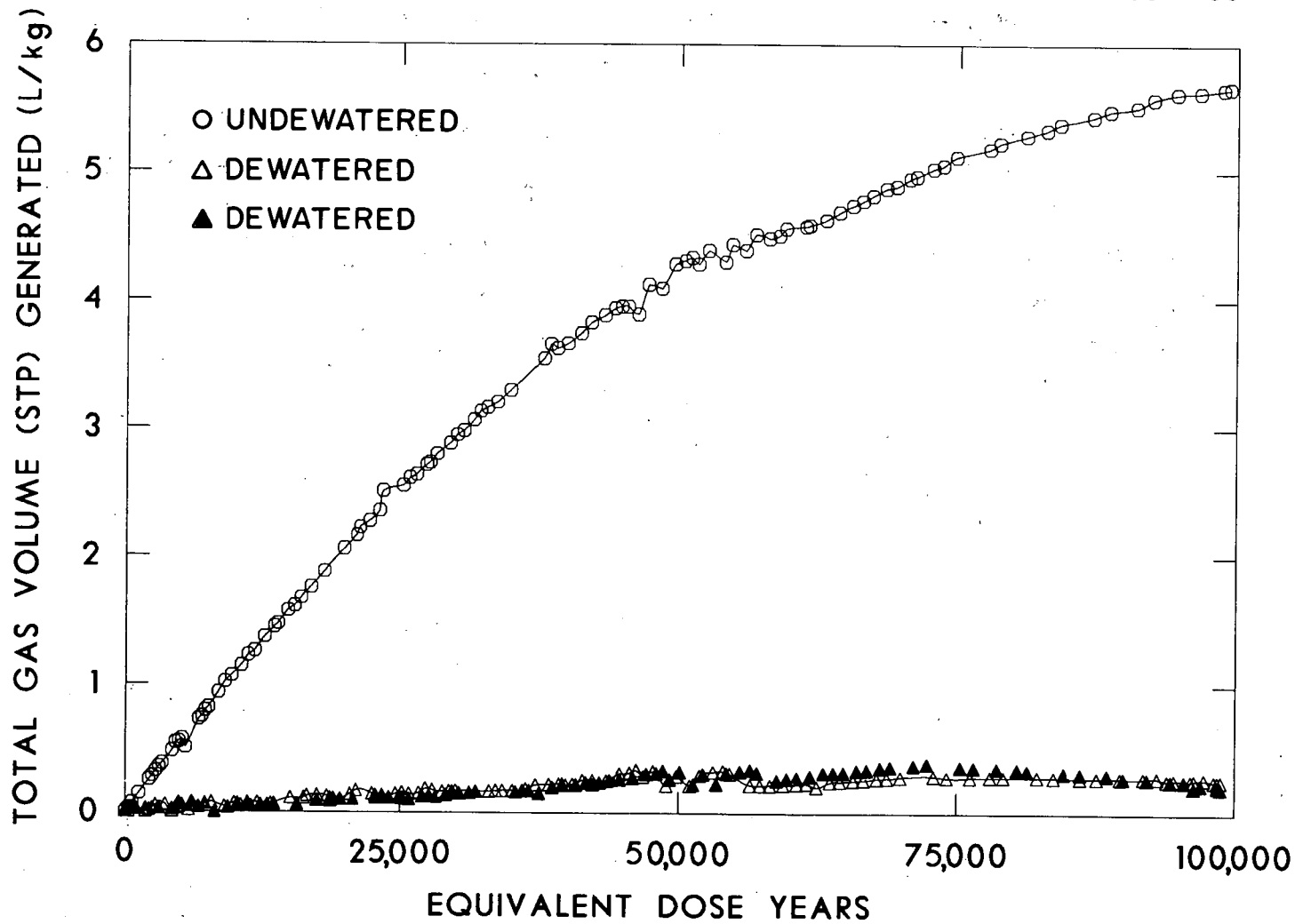


Fig. 27. Comparison of gas generation rates of SRP FUEAP concrete before and after dewatering.

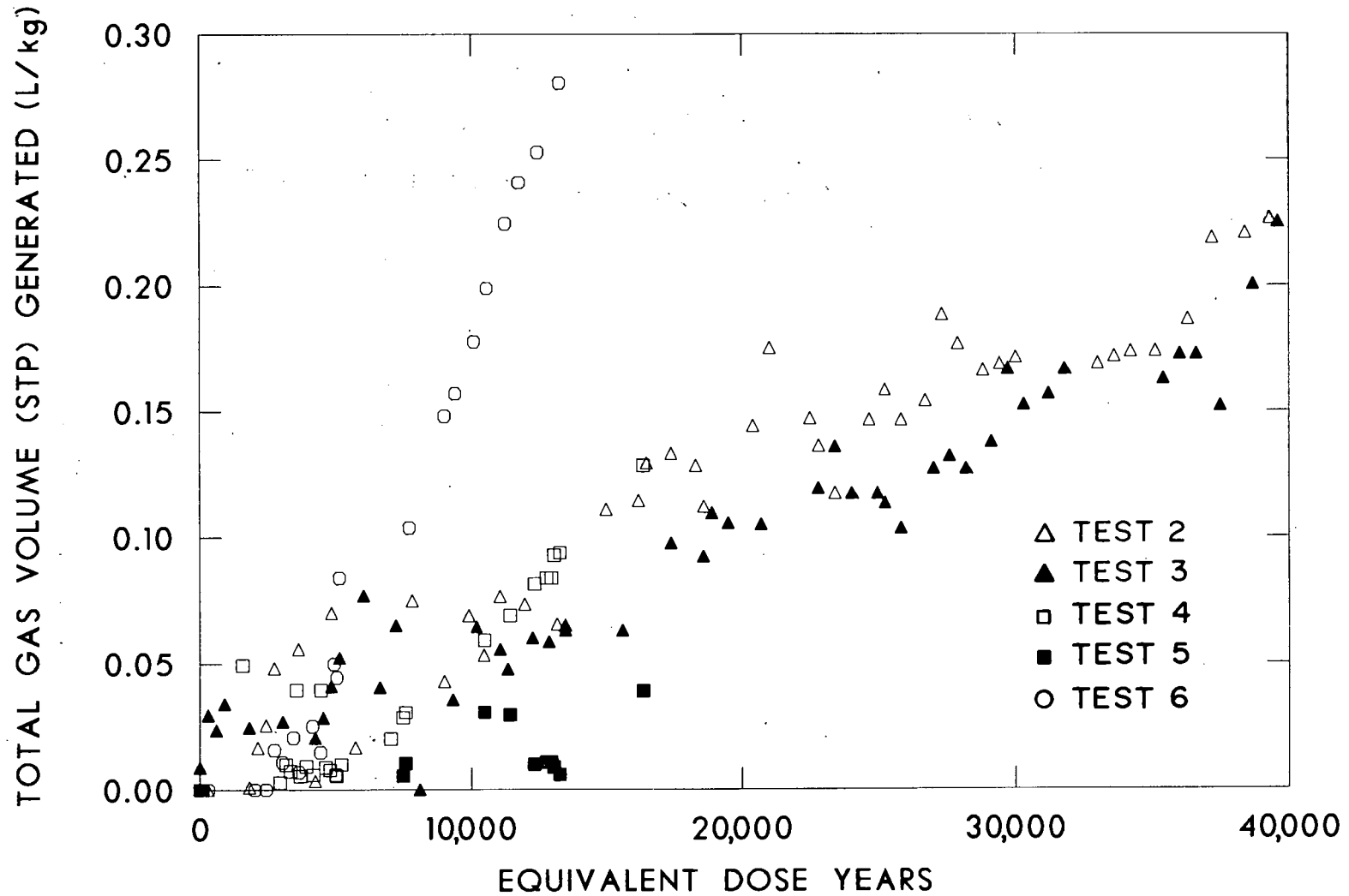


Fig. 28. Comparison of all gas generation rates of dewatered FUETAP concretes (tests 2 through 6).

concretes. In much shorter tests (200 h) performed by Kazanjian and Killion,²⁸ nitrogen was also shown to be a major radiolysis product in nitrate-containing, dewatered Rocky Flats Building 774 sludge.

Table 17. Composition^a of gases generated in alpha-radiolysis tests of FUETAP concrete specimens

Compound	Test			
	1 ^b	1 ^c	2	3
H ₂	46.49	49.60	0.59	0.24
He	1.64	0.05	1.57	0.17
CH ₄	0.01	0.01	0.02	0.01
N ₂ + CO	18.21	10.10	96.15	30.62
O ₂	33.10	39.88	1.32	0.20
Ar	0.15	0.03	0.33	68.75
CO ₂	0.40	0.33	0.02	0.01

^aMass spectrometric analysis in vol %.

^bGas sample taken after 500 d.

^cGas sample taken after 860 d.

8. IMPACT STRENGTH

The FUETAP concretes are high-strength products (compressive strength, 40 to 100 MPa). MCC-1 impact tests²⁹ performed on a specimen with a geometric surface area of $2.58 \times 10^{-2} \text{ m}^2$ at an energy of 10 J/cm^3 caused no measurable increase in BET surface area. A mass fraction of 0.3 to 0.4% of respirable fines (i.e., $<10 \text{ }\mu\text{m}$) was generated by the tests (Fig. 29). There was essentially no difference in the results for specimens cured at 100°C and those prepared at 250°C .

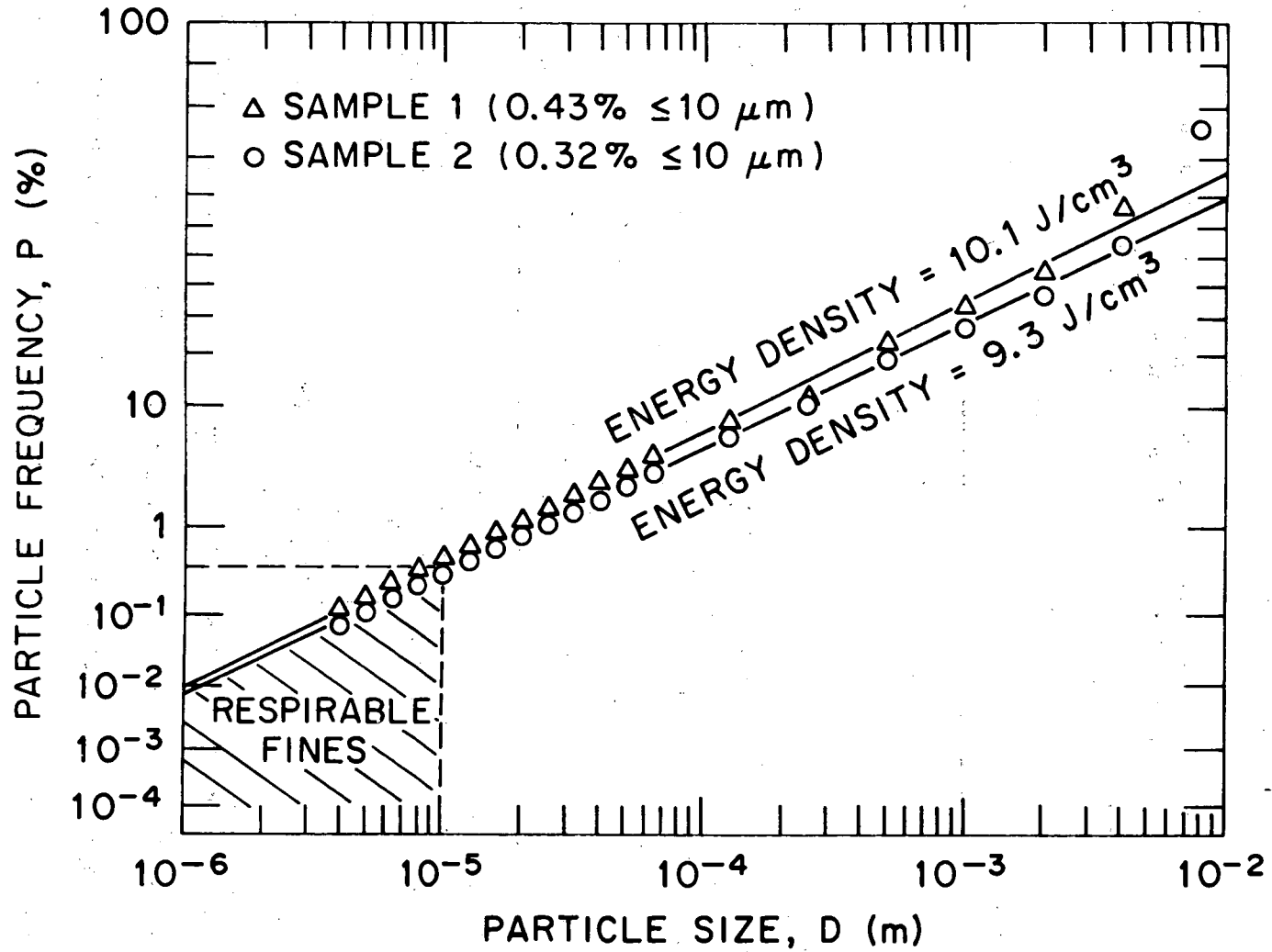


Fig. 29. Dynamic impact test of SRP FUETAP concrete specimens.

9. SUMMARY

As a radioactive waste form, the FUETAP concretes show dynamic leach rates of transuranics below detectable limits [$0.01 \text{ g}_i/(\text{m}^2 \cdot \text{d})$]. Cesium and strontium leachabilities compare with those for glass; however, the initial washout is higher, and it usually dominates the short-term (28-d) results.

Radiolytic decomposition of these low-water ($<2 \text{ wt } \%$) FUETAP concretes is negligible over accelerated time tests to $>10^5$ years. They are thermally stable to 900°C and exhibit less thermal expansion than steel.

The FUETAP concretes are high-strength products (compressive strength, 40 to 100 MPa); less than 0.4 wt % respirable fines is generated upon impact of $\sim 10 \text{ J/cm}^3$. Their porosities and permeabilities are directly proportional, while the thermal conductivities and densities are inversely proportional, to the formula's water/cement (w/c) ratio. This w/c ratio depends on the allowable rheological limits and the water demand of the specific process waste stream. The FUETAP concrete must be tailored as an engineered buffer between the specific waste stream and the disposal environment.

Concretes have been the principal hosts for most low- and intermediate-level wastes for three decades. Since accelerated curing is also a common industrial practice, no inventions are required to apply the FUETAP process. By using inexpensive and readily available materials and requiring low processing temperatures, it allows a wide latitude of formulations and therefore accommodates a broad range of waste streams.

The combined cementitious and radwaste phases are complex mixtures. Identification of these phases, together with the location of the specific nuclides, has just begun. Extensive testing has confirmed that FUETAP concretes can serve as durable, tenacious hosts for most of the major defense and reprocessing, radioactive waste streams. The questions with regard to phase characterization are fostered by an intense curiosity as to why they work so well.

This study shows that FUETAP concretes have excellent possibilities as waste hosts for high-level radioactive wastes.

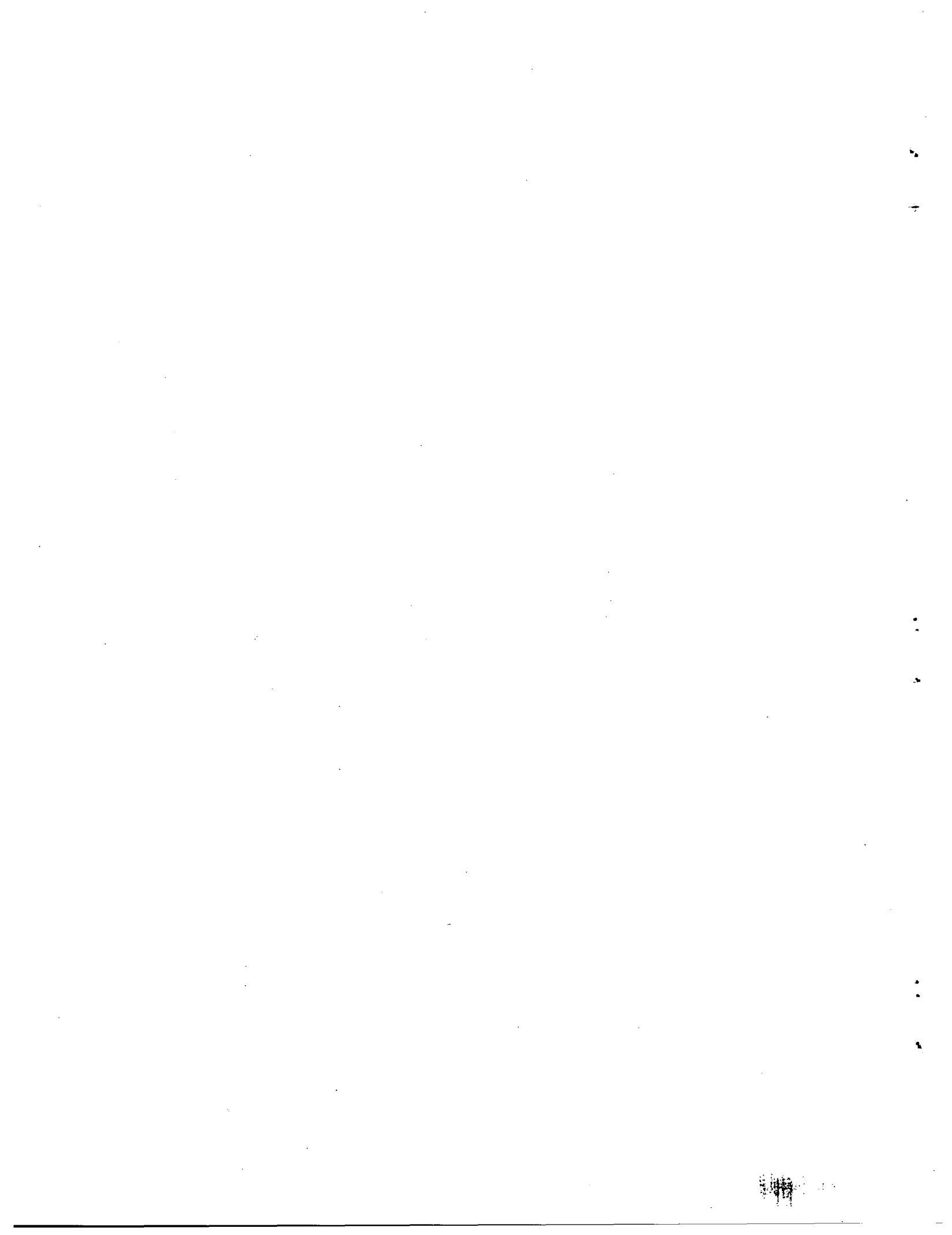
10. REFERENCES

1. R. O. Lokken, A Review of Radioactive Waste Immobilization in Concrete, PNL-2654 (June 1978).
2. A. H. Kibbey and H. W. Godbee, A Critical Review of Solid Radioactive Waste Practices at Nuclear Power Plants, ORNL-4924 (March 1974).
3. H. O. Weeren, "Waste Disposal by Shale Fracturing at ORNL," Nucl. Eng. Des., 44, 291-300 (1977).
4. J. G. Moore, H. W. Godbee, A. H. Kibbey, and D. S. Joy, Development of Cementitious Grouts for the Incorporation of Radioactive Wastes. Part I: Leach Studies, ORNL-4962 (April 1975).
5. J. G. Moore, Development of Cementitious Grouts for the Incorporation of Radioactive Wastes. Part 2: Continuation of Cesium and Strontium Leach Studies, ORNL-5142 (September 1976).
6. J. G. Moore et al., p. 277 in Proceedings of the Symposium on Waste Management, Waste Management 1981 Conference, Vol. 1, R. G. Post, ed., Tucson, Arizona, 1971.
7. D. M. Roy and G. G. Gouda, "High Level Radioactive Waste Incorporation into Special Cements," Nucl. Technol., 40, 214-19 (September 1978).
8. W. E. Clark, "The Isolation of Radioiodine with Portland Cement. Part 1: Scoping Leach Studies," Nucl. Technol., 36, 215-21 (1977).

9. M. T. Morgan, J. G. Moore, H. E. Devaney, G. C. Rogers, C. Williams, and E. Newman, "The Disposal of Iodine-129," in Proceedings of the Scientific Basis for Nuclear Waste Management, Boston, Mass., G. J. McCarthy, ed., Plenum Press, New York, 1979.
10. J. G. Moore et al., in Proceedings of the International Seminar on Chemistry and Process Engineering for High-Level Liquid Waste Solidification, Kernforschungsanlage, Julich, Federal Republic of Germany, 1981.
11. J. G. Moore, p. 194 in Proceedings of a Workshop on Alternative Nuclear Waste Forms and Interactions in Geologic Media, CONF-8005107, L. A. Boatner and G. C. Battle, Jr., eds., Technical Information Center, Oak Ridge, Tenn., 1981.
12. J. G. Moore, E. Newman, and G. C. Rogers, Radioactive Waste Fixation in FUETAP (Formed Under Elevated Temperatures and Pressure) Concrete Experimental Program and Initial Results, ORNL/TM-6573 (March 1979).
13. J. G. Moore et al., p. 132 in Proceedings of the Conference on Ceramics in Nuclear Waste Management, CONF-790420, T. D. Chikalla and J. E. Mendel, eds., Technical Information Center, Oak Ridge, Tenn., 1979.
14. R. G. Post, Panel Chairman, Independent Review Panel to Evaluate and Review Alternative Waste Forms to Immobilize the Idaho Chemical Processing Plant (ICPP) Waste: Final Report, ENICO-1088, Exxon Nuclear Idaho Co., Idaho Falls, Idaho, 1971.
15. H. O. Weeren and J. J. Perona, A Preliminary Engineering and Economic Analysis of the Fixation of High-Level Radioactive Waste in Concrete, ORNL/TM-6863 (July 1979).
16. E. R. Johnson Associates, Inc., Preliminary Evaluation of Alternative Waste Form Solidification Processes, Vol. II: Evaluation of the Processes, PNL-3477, Pacific Northwest Laboratory, Richland, Wash., 1980.
17. J. A. Stone et al., Preliminary Evaluation of Alternative Forms for Immobilization of Savannah River Plant High-Level Waste, DP-1545 (December 1979).
18. L. R. Dole et al., Leach and Radiolysis Data for FUETAP Concrete Containing SRP Wastes, ORNL/TM-8579/S1 (Suppl.), in press.
19. J. G. Moore, M. T. Morgan, E. W. McDaniel, H. B. Greene, and G. A. West, Cement Technology for Plugging Boreholes in Radioactive Waste Repository Sites: Progress Report for the Period October 1, 1977 to September 30, 1978, ORNL-5524 (August 1979).
20. Materials Characterization Center MCC-1 Static Leach Test (Draft), Pacific Northwest Laboratory, Richland, Wash. (January 1981).

21. J. G. Moore, H. W. Godbee, and A. H. Kibbey, Nucl. Technol., 32, 39 (January 1977).
22. D. M. Strachan, B. O. Barnes, and R. P. Turcotte, p. 341 in Conference on the Scientific Basis for Nuclear Waste Management, Vol. 3, J. G. Moore, ed., Plenum Press, New York, 1981.
23. H. W. Godbee et al., "Application of Mass Transport Theory to the Leaching of Radionuclides from Waste Solids," Nucl. Chem. Waste Manage. 1, 29 (1980).
24. J. A. Stone, Evaluation of Concrete as a Matrix for Solidification of Savannah River Plant Waste, DP-1448 (June 1977).
25. N. E. Bibler, Radiolytic Gas Production from Concrete Containing Savannah River Plant Waste, DP-1464 (January 1978).
26. N. E. Bibler, pp. 585-92 in Proceedings of the Conference on the Scientific Basis for Nuclear Waste Management, Vol. 2, C. J. M. Northrup, ed., Plenum Press, New York, 1980.
27. S. Katz, pp. 577-84 in Proceedings of the Conference on the Scientific Basis for Nuclear Waste Management, Vol. 2, J. G. Moore, ed., Plenum Press, New York, 1980.
28. A. R. Kazanjian and M. E. Killion, Radiolytic Gas Generation from Sludge, CRD 81-025, Rockwell International, Rocky Flats, Colo., 1981.
29. L. J. Jardine et al., Final Report of Experimental Laboratory-Scale Brittle Fracture Studies of Glasses and Ceramics, ANL-82-39 (October 1982).

11. APPENDIXES



Appendix A: Compositions and Properties of SRP FUETAP Concretes

This appendix details the compositions of the concrete mixes (Table A.1) and the simulated wastes incorporated in these mixes (Table A.2) for use in the SRP FUETAP program. Physical properties for various SRP formulations are also given (Table A.3).

Table A.1. Compositions of SRP FUETAP concretes^a

Component	FUETAP concrete formulation							
	MCC-1 ^h	MCC-2	MCC-3	MCC-4	MCC-5	MCC-6A	MCC-6B	SRPZ9
Cement	22.0	24.0	22.0	22.0	22.0	22.0	22.0	25.0
I.R. clay ^b	-	-	7.0	3.5	-	3.5	-	-
Bent. clay ^c	-	-	-	3.5	-	-	3.5	-
Fly ash ^d	11.0	12.0	11.0	11.0	11.0	11.0	11.0	12.5
SRP waste ^e	20.0	15.0	20.0	20.0	20.0	20.0	20.0	20.0
Sand	27.75	29.75	20.75	20.75	26.75	23.25	23.25	27.0
Water	18.0	18.0	18.00	18.0	19.00	19.0	19.0	14.5
D-65 ^f	1.25	1.25	1.25	1.25	1.25	1.25	1.25	1.0
CFR-18	-	-	-	-	0.05	0.02	0.02	-

^aValues are given in wt %.

^bIndian red pottery clay.

^cBentonite clay.

^dFly ash from Kingston, Tenn.

^eCompositions are listed in Table A.2. SRP-4 waste was generally used in FUETAP concrete specimens MCC-1 through MCC-5; SRP-6 waste was used in specimens MCC-6A and MCC-6B.

^fWater reducer from Dowell Division of Dow Chemical, Houston, Tex.

^gDelta gluconolactone set regulator obtained from Halliburton Services, Inc. of Duncan, Oklahoma.

^hMCC-1 is used to identify both a Materials Characterization Center static leach test and a specific SRP FUETAP concrete formulation.

Table A.2. Compositions of simulated SRP wastes^a

Component	Simulated SRP waste ^b					
	SRP-1 ^c	SRP-2 ^d	SRP-3 ^e	SRP-4 ^f	SRP-5 ^g	SRP-6 ^g
Fe ₂ O ₃	38.4	36.1	39.0	47.2	51.3	49.9
Al ₂ O ₃	6.8	28.2	31.0	9.2	10.1	9.8
MnO ₂	17.1	9.9	10.9	13.0	14.1	13.7
U ₃ O ₈	-	-	-	-	-	4.5
PbO ^h	16.5	3.2	3.6	-	-	-
CeO ₂ ^h	2.5	-	-	2.1	2.3	-
Gd ₂ O ₃ ^h	-	-	-	2.1	2.3	-
CaO	1.0	2.7	3.0	2.5	3.8	3.7
NiO	6.5	4.4	4.9	5.9	6.4	6.2
SiO ₂	-	0.8	1.0	1.1	1.2	1.2
Na ₂ O	-	5.0	5.6	6.6	7.2	7.0
Na ₂ SO ₄	7.0	0.9	1.0	1.2	1.3	1.3
NiO	6.5	-	-	-	-	-
Cr ₂ O ₃	0.5	-	-	-	-	-
BaO ₂	0.3	-	-	-	-	-
NaF	2.0	-	-	-	-	-
Na ₂ HPO ₄	1.4	-	-	-	-	-
Nd ₂ O ₃ ⁱ	-	-	-	-	-	1.1
Ce ₂ O ₃ ⁱ	-	-	-	-	-	1.1
SrO ⁱ	-	-	-	1.0	-	0.5
Zeolite ^j	-	8.9	-	8.1	-	-

^aMajor elements are given in wt %.

^bThese compositions were according to SRP program guidelines, which reflect their flowsheet modifications during the course of the program.

^cSimulated wastes used in initial FUETAP tests.

^dComposite SRP waste without aluminum removal.

^eComposite SRP waste without aluminum removal adjusted for no zeolite.

^fComposite SRP waste with aluminum removal.

^gComposite SRP waste with aluminum removal adjusted for no zeolite.

^hModified formula using uranium substitutes in accordance with SRP's request.

ⁱModified formula incorporating strontium, cerium, and neodymium in accordance with SRP's request.

^jThe zeolite Ionsiv IE-95 was loaded with cesium equivalent to a Cs₂O loading of 12.4 wt % so that the final waste solids would contain 1 wt % cesium.

Table A.3. Physical properties of SRP FUEAP concretes

Mix	Waste	Dewatered density (g/cm ³)	Thermal conductivity [W/(m·K)]	Porosity (%)	Sand (wt %)	Water/cement ratio
MCC-1	SRP-4	1.79	0.85	35.1	27.8	0.818
MCC-1	SRP-4	1.81	0.88	34.6	27.8	0.818
MCC-1	SRP-4	1.82	0.89	34.0	27.8	0.818
MCC-1	SRP-4	1.85	0.88	32.7	27.8	0.818
MCC-1	SRP-4	1.88	0.90	30.4	27.8	0.818
MCC-1	SRP-4	1.91	0.94	29.5	27.8	0.818
MCC-1	SRP-4	1.45	-	-	27.8	0.818
MCC-1	SRP-4	1.49	-	-	27.8	0.818
MCC-1	SRP-4	2.09	-	-	27.8	0.818
MCC-1	SRP-4	1.80	-	-	27.8	0.818
MCC-2	SRP-4	1.94	0.95	26.9	29.8	0.75
MCC-3	SRP-4	2.49	-	-	20.8	0.818
MCC-4	SRP-4	2.27	-	-	20.8	0.818
MCC-6A	SRP-6	1.72	0.65	34.7	27.0	0.864
MCC-6B	SRP-6	1.72	0.49	41.4	27.0	0.864
a	SRP-1	1.39	0.44	-	0	1.02
a	SRP-1	1.41	0.46	-	0	1.02
a	SRP-1	1.42	0.48	-	0	0.73
a	SRP-1	1.42	0.47	-	0	1.02
a	SRP-1	1.42	0.47	-	0	1.02
a	SRP-1	1.44	0.48	-	0	0.73
a	SRP-2	1.44	0.48	-	0	1.02
a	SRP-2	1.50	0.48	-	0	0.94
a	SRP-4	1.88	1.00	-	29.5	0.68

^aTests made early in program using experimental mix formulations.

Appendix B: Statistical Analysis of Uranium MCC-1 Leach Tests

The statistical analysis of 70 uranium MCC-1 leach tests is summarized in this appendix. Table B.1 shows that there was a significant difference in uranium concentrations (ppm) between waste formulas SRP-6A and SRP-6B, which contained 3.5% Indian red pottery clay and bentonite clay, respectively. However, no significant time dependence of the uranium concentrations (ppm) is apparent. Table B.2 shows that there was no statistically significant difference in uranium solubilities between deionized water (DIW) and silica-water (SIW) leachants. However, the MCC-1 brine leachant (BRI) held more uranium in solution. This information confirms that the MCC-1 test does not measure leaching, but only uranium solubility, which was found to be the same at 40 and 90°C in MCC-1 brine (BRI) (Table B.2). As noted in Table B.2, there was an increase in solubility with temperature in the MCC-1 silica water (SIW).

Table B.1. Duncan's multiple range test^a - uranium vs variable shown
 Alpha = 0.05; DF = 66; MSE = 0.0244771^b
 [Means with the same letter (e.g., A) are not significantly different]

Variable	Duncan grouping	Harmonic mean of cell sizes	Mean	N	Waste	Leaching time (d)	Leach
Waste formula	A	34.5429	0.16027	39	SRP-6B ^c	-	-
	B	34.5429	0.03877	31	SRP-6A	-	-
Days leached	A	5.69637	0.15214	10	-	3	-
	A	5.69637	0.10635	53	-	28	-
	A	5.69637	0.04583	3	-	7	-
	A	5.69637	0.03932	4	-	14	-
Leachant	A	23.1555	0.24468	21	-	-	BRI ^d
	B	23.1555	0.060207	23	-	-	DIW ^e
	B	23.1555	0.03576	26	-	-	SIW ^f

^aThis test controls error rates at different levels depending on the number of means between each pair compared. Its operating characteristics are somewhat similar to those of Fisher's unprotected LSD test. D. B. Duncan, "t-Tests and Intervals for Comparisons Suggested by the Data," Biometrics 31, 339-59 (June 1975).

^bAlpha = the level of significance; DF = error degrees of freedom; and MSE = error mean squares.

^cComposition given in Appendix A.

^dBRI = salt brine.

^eDIW = quartz distilled water.

^fSIW = silica water.

Table B.2. Duncan's multiple range test^a for uranium concentration (ppm) vs temperature

(Means with the same letter are not significantly different)

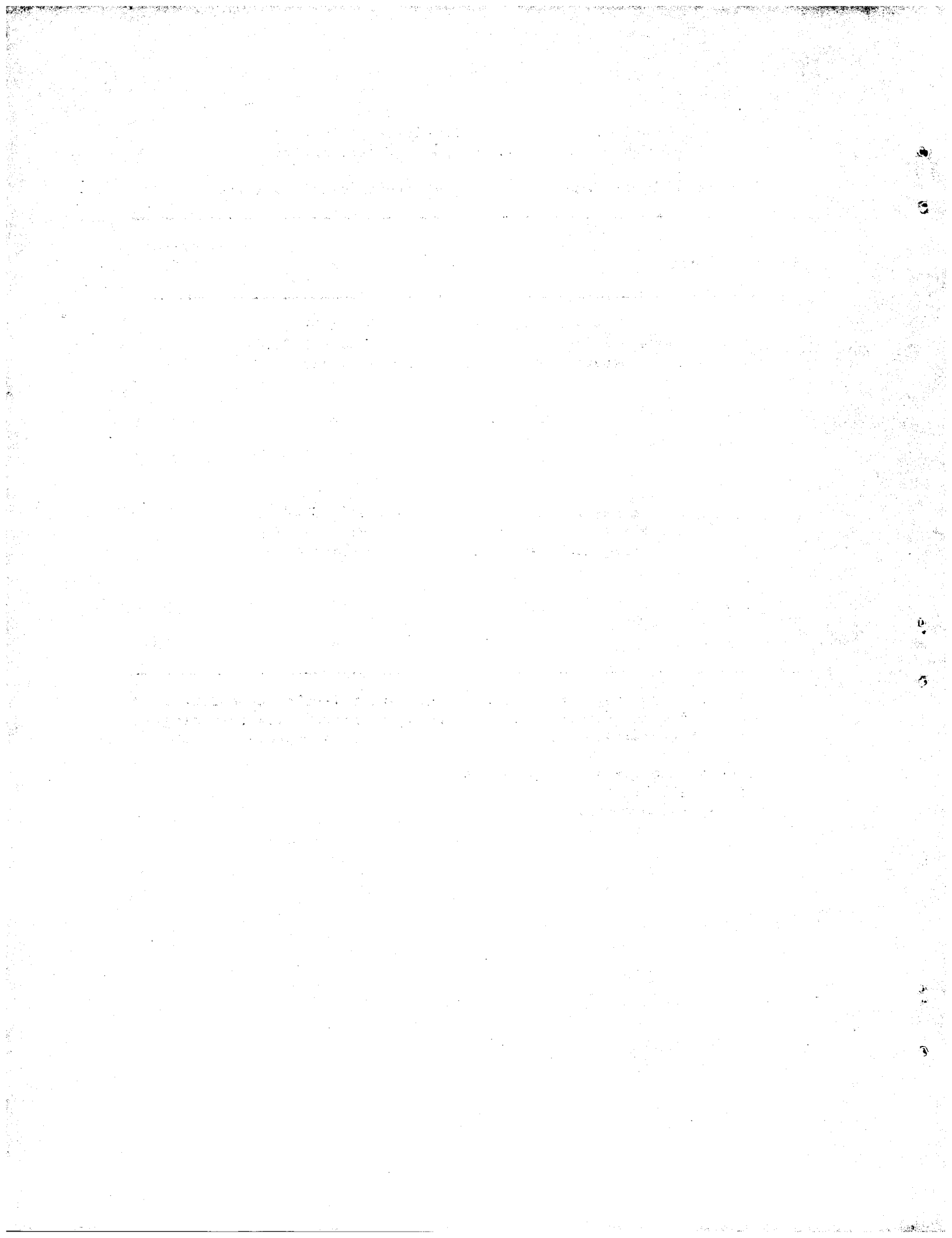
Duncan grouping	Mean	N	Temperature (°C)
On waste formula SRP6A ^b leached in BRI ^c Alpha = 0.05 DF = 5 MSE = 2.0E-04 Harmonic mean of cell sizes = 3.42857.			
A	0.076650	4	90
A	0.171767	3	40
On Waste formula SRP6A ^b leached in SIW ^d Alpha = 0.05 DF = 11 MSE = 2.1E-04 Harmonic mean of cell sizes = 6.46154			
A	0.032529	7	90
B	0.011850	6	40

^aThis test controls error rates at different levels, depending on the number of means between each pair being compared. Its operating characteristics somewhat resemble those of Fisher's unprotected LSD test.

^bComposition given in Appendix A.

^cBRI = salt brine.

^dSIW = silica water.



INTERNAL DISTRIBUTION

- | | | | |
|--------|-------------------|--------|----------------------------|
| 1. | J. O. Blomeke | 25. | W. W. Pitt |
| 2-6. | L. R. Dole | 26-30. | S. M. Robinson |
| 7. | C. W. Forsberg | 31-35. | G. C. Rogers |
| 8. | J. R. Gissel | 36. | T. H. Row |
| 9. | H. W. Godbee | 37. | F. M. Scheitlin |
| 10. | F. A. Kappelmann | 38. | J. D. Sease |
| 11-15. | J. H. Kessler | 39. | J. H. Stewart, Jr. |
| 16. | E. M. King | 40. | M. G. Stewart |
| 17. | A. H. Kibbey | 41-45. | D. P. Stinton |
| 18. | W. J. Lackey | 46. | H. O. Weeren |
| 19. | G. F. Larson | 47. | G. A. West |
| 20. | R. S. Lowrie | 48. | S. K. Whatley |
| 21. | A. P. Malinauskas | 49-50. | Central Research Library |
| 22. | E. W. McDaniel | 51. | Document Reference Section |
| 23. | K. J. Notz | 52-53. | Laboratory Records |
| 24. | M. M. Osborne | 54. | Laboratory Records - RC |
| | | 55. | ORNL Patent Office |

EXTERNAL DISTRIBUTION

56. Office of Assistant Manager for Energy Research and Development, DOE-ORO, P. O. Box E, Oak Ridge, Tennessee 37830.
57. D. E. Large, DOE-ORO, P. O. Box E, Oak Ridge, Tennessee 37830.
58. M. T. Morgan, 109 N. Purdue, Oak Ridge, Tennessee 37830.
- 59-61. J. G. Moore, 517 Vista Drive, Oak Ridge, Tennessee 37830.
62. Della Roy, Pennsylvania State University, Materials Research Laboratory, University Park, Pennsylvania 16802.
63. Mary Barnes, Pennsylvania State University, Materials Research Laboratory, University Park, Pennsylvania 16802.
64. Barry Scheetz, Pennsylvania State University, Materials Research Laboratory, University Park, Pennsylvania 16802.
65. Martin J. Steindler, Argonne National Laboratory, 9700 S. Cass Avenue, Argonne, Illinois 60439.
66. W. H. Beers, EG&C Idaho, Willow Creek Building, P. O. Box 1625, Idaho Falls, Idaho 83415.

67. J. H. Campbell, Lawrence Livermore National Laboratory, University of California, P. O. Box 808, Livermore, California 94550.
68. R. H. Campbell, DOE, Albuquerque Operations Office, Actions Office, P. O. Box 5400, Albuquerque, New Mexico 87115.
69. W. Carbiener, Office of Nuclear Waste Isolation, Battelle Project Office, 505 King Avenue, Columbus, Ohio 43201.
70. T. D. Chikalla, Battelle-Pacific Northwest Laboratory, P. O. Box 999, Richland, Washington 99352.
71. F. R. Cook, Nuclear Regulatory Commission HLW Licensing Branch, Materials Section, Washington, DC 20555.
72. W. R. Cornman, Savannah River Laboratory, P. O. Box A, Aiken, South Carolina 29801.
73. M. W. Davis, University of South Carolina, Columbia, South Carolina 29208.
74. J. L. Deichman, Rockwell Hanford Operations, Energy Systems Group, P. O. Box 800, Richland, Washington 99352.
75. K. V. Gilbert, Transuranic Waste Systems Office, Rockwell International, P. O. Box 464, T690B, Golden, Colorado 80401.
76. H. Groh, E. I. duPont de Nemours & Co., Inc., Savannah River Plant, Aiken, South Carolina 29801.
77. J. P. Hamric, Idaho Operations Office, DOE, 550 Second St., Idaho Falls, Idaho 83401.
78. S. G. Harbinson, San Francisco Operations, DOE, P. O. Box 5400, Albuquerque, New Mexico 87115.
79. E. C. Hardin, Albuquerque Operations Office, DOE, P. O. Box 5400, Albuquerque, New Mexico 87115.
80. L. L. Hench, Department of Materials Science & Engineering, University of Florida, Gainesville, Florida 32611.
81. E. J. Hennelly, Savannah River Laboratory, P. O. Box A, Aiken, South Carolina 29801.
82. T. Hindman, Waste Management Program Office, Savannah River Operations Office, DOE, P. O. Box A, Aiken, South Carolina 29801.
83. L. J. Jardine, Bechtel National, Inc., P. O. Box 3965, Mail Stop 45/16/D20, San Francisco, California 94119.

84. K. H. Kittel, Office of Waste Management Programs, Argonne National Laboratory, 9700 South Cass Ave., Argonne, Illinois 60439.
85. J. L. Landon, Richland Operations Office, DOE, P. O. Box 550, Richland, Washington 99352.
86. R. Y. Lowrey, Weapons Production Division, DOE, Albuquerque, Operations Office, P. O. Box 5400, Albuquerque, New Mexico 87115.
87. P. B. Macedo, Catholic University of America, Washington, DC 20017.
88. N. J. Magnani, Sandia National Laboratory, Department 5840, P. O. Box 5800, Albuquerque, New Mexico 87115.
89. S. A. Mann, Chicago Operations and Regional Office, DOE, Argonne, Illinois 60439.
90. D. E. McKenzie, Rockwell Energy Systems Group, P. O. Box 800, Richland, Washington 99352.
91. J. E. Mendel, Pacific Northwest Laboratory, P. O. Box 999, Richland, Washington 99352.
92. S. Mirshak, Savannah River Laboratory, P. O. Box A, Aiken, South Carolina 29801.
93. J. O'Keefe, Goddard Space Flight Center, Greenbelt, Maryland 20770.
94. H. Palmour, III, 2140 Burlington Engineering Laboratories, North Carolina State University, Raleigh, North Carolina 27607.
95. W. A. Ross, Nuclear Process Technology and Analysis Section, Battelle Pacific Northwest Laboratories, P. O. Box 999, Richland, Washington 99352.
96. R. Roy, Materials Research Laboratory, Pennsylvania State University, University Park, Pennsylvania 16802.
97. J. T. Schreiber, Waste Management Division, Richland Operations Office, DOE, Richland, Washington 99352.
98. J. B. Whitsett, Nuclear Fuel Cycle Division, DOE, Idaho Operations Office, 550 Second Street, Idaho Falls, Idaho 83401.
99. W. B. Wilson, Waste Management Program Office, Savannah River Operations Office, DOE, P. O. Box A, Aiken, South Carolina 29801.

DOE - Oak Ridge Operations, Oak Ridge, Tennessee 37830

100. D. R. Brown

101. M. M. Dare

102. E. L. Keller

103. Director, Nuclear Research and Development Division.

DOE - MS-B-107, Washington, DC 20545

104. W. Ballard, Jr., NE-330, GPN.

105. C. R. Cooley, NE-331, Office of Waste Operations and Technology.

106. G. H. Daly, Technology Division, Office of Waste Operations and Technology.

107. J. E. Diekhoner, Operations Division, Office of Waste Operations.

108. D. J. McGaff, Projects Division, Office of Waste Operations.

109. G. K. Oertel, Office of Waste Operations.

110. A. Perge, Office of Deputy Assistant Secretary for Nuclear Waste Management.

111. R. D. Walton, Technology Division, Office of Waste Operations.

112-424. Given distribution as shown in TIC-4500 under Nuclear Waste Management category (25 copies - TIC).